TRANSIENT THERMODYNAMIC ANALYSIS OF GENERATOR IN A SOLAR ABSORPTION SYSTEM DESIGNED FOR HOT AND HUMID REGIONS

BY
HAMZA KAMAL ALI MUKHTAR

A Thesis Presented to the
DEANSHIP OF GRADUATE STUDIES

KING FAHD UNIVERSITY OF PETROLEUM & MINERALS

DHAHRAN, SAUDI ARABIA

In Partial Fulfillment of the
Requirements for the Degree of

MASTER OF SCIENCE

In

MECHANICAL ENGINEERING

December 2016

IN THE NAME OF ALLAH, THE MOST GRACIOUS AND THE MOST MERCIFUL

KING FAHD UNIVERSITY OF PETROLEUM & MINERALS

DHAHRAN- 31261, SAUDI ARABIA

DEANSHIP OF GRADUATE STUDIES

This thesis, written by **HAMZA KAMAL ALI MUKHTAR** under the direction of his thesis advisor and approved by his thesis committee, has been presented and accepted by the Dean of Graduate Studies, in partial fulfillment of the requirements for the degree of **MASTER OF SCIENCE IN MECHANICAL ENGINEERING.**

Dr. Zuhair M. A. Gasem
Department Chairman

Dr. S. A. M. Said
(Advisor)

Dr. Salam A. Zummo
Dean of Graduate Studies

Dr. Amro Al-Qutub
(Member)

28/2/17

Date

15/11/2017

Dr. Fahad A. Al-Sulaiman
(Member)

Declaration

By electronically submitting this research, I announce that the totality of this work is my own, originally, that I am the solo author there-of (unless evidently otherwise stated), that re-production or publication thereof by KFUPM won't trespass rights of any third party.

DEDICATED TO THE SPIRIT OF MY FATHER, MY BELOVED MOTHER, MY ONE & ONLY SISTER, MY DEAR BROTHERS AND MY TRUTHFUL FRIENDS WHOM I CAN'T DISPENSE WITH THEM.

ACKNOWLEDGMENTS

Firstly, I would like to thank the almighty Allah for giving me the ability and patient to accomplish this work, to reach this special moment of self-satisfaction.

Then, I would like to acknowledge those who have contributed in my Master Thesis, without their involvement, this research would have never finished.

I really appreciate Dr. Maged El-Shaarawi for his guidance, advices, ideas, and suggestions have been essential for enhancing this study. Here also I would thanks my advisor Dr. Syed Said for his essential role. His continuous support is highly appreciated, beside his corrections that have fundamental roles in this thesis.

In addition, I would also not to forget Dr. Amro Al-Qutub and Dr. Fahad A. Al-Suliman for their time, revising this work, and giving me helpful practical comments and facts about solar and absorption systems.

Last not least, I would finish this acknowledgement with a great thank to my whole family and friends. Without them I would never have stood on this platform. The endless support and the hopefulness transmitted from my mother, lovely sister, and my dear brothers throughout all these years have been the driving-force to accomplish my aims and achieve my targets, encompassing this project. Also, never to forget all my friends back at home for continuous support and encouragement.

TABLE OF CONTENTS

LIST OF TABLES

LIST OF FIGURES

LIST OF ABBREVIATIONS

A_c	:	Area of Solar collector (m^2)
AU	:	Heat transfer coefficient (kW/°C)
F'		Efficiency factor
F"		Collector-flow factor
F_R	:	Heat-removal factor
h	:	specific enthalpy (kj/kg)
I	:	Solar radiation per unit area (kW/m^2)
M	:	Solution mass
$\dot{m}$	:	Mass flow rate (kg/s)
Q	:	Heat transfer rate (kW)
Q_u	:	Useful heat gain from the collector (kW)
T	:	Temperature (°C)
t	:	Time (s)
U	:	Total energy of the solution (kj)
U	:	Overall heat transfer coefficient of the collector (kW/m^2)
u	:	specific internal energy (kj/kg)
W	:	Work (kW)
X	:	LiBr concentration in the solution (%)

Greek symbols

α	:	Absorptivity
τ	:	Transitivity
ε	:	Effectiveness

Subscripts

A	:	Absorber
a	:	Ambient
C	:	Condenser
cr	:	Crystallization
E	:	Evapoartor
G	:	Generator or Desorber
in		inlet
l	:	Losses
out		outlet
p	:	Pump
s	:	Solution
st	:	Structure of the component
w		water

Abbreviations

COP	:	*Coefficient of performance*
ETC	:	Evacuated tube collector
FPC	:	Flat plat collectors
REV	:	Refrigerant expansion valve
SAT	:	Single-axis tracking collector
SEV	:	Solution expansion valve
TR	:	Ton of Refrigeration

ABSTRACT

FULL NAME : HAMZA KAMAL ALI MUKHTAR

THESIS TITLE : TRANSIENT THERMODYNAMIC ANALYSIS OF GENERATOR IN A SOLAR ABSORPTION SYSTEM DESIGNED FOR HOT AND HUMID REGIONS

MAJOR FIELD : MECHANICAL ENGINEERING

DATE OF DEGREE : DECEMBER, 2016

This research presents development of a dynamic-model for a single effect absorption cooling cycle that employs LiBr/water as an absorbent/refrigerant pair by executing a transient thermodynamic analysis. Problems related to Carbon Dioxide CO_2 emissions motivate researchers in the engineering area to focus on alternatives to the conventional sources of power or enhance the existing ones. Accordingly, a lot of studies and experiments, have been conducted on the absorption systems to understand its actual performance minutely to improve it and increase its Coefficient of Performance (COP). In this regard, even if the input power is controlled, there will be a transient period that precedes the steady operation period of the machine due to the initial mass unbalance inside absorption system components. Throughout this unsteady stage, most parameters keep fluctuating and do not stabilize at particular values, and some of them may go away of their allowed ranges in a manner that affect the machine performance severely. This phenomena is considered as a prime motivation and fundamental concern of this study. The dynamic model is based on mass, momentum, and energy balances while taking into account the dynamic response of the cycle with special focus on the generator performance which supposed to be driven by means of solar field.

The results indicate that it takes an average of 14 minutes before most of parameters stabilize at their operating values and the dynamic terms fade away in what so called steady-state

operation. Then, the developed model was verified with a dynamic model reported in the literature, as well as another in steady state condition. The comparison reveals an acceptable agreement with both. After that, the applied initial values were optimized to avoid the risk of crystallization throughout the operation. Furthermore, the effects of the heat input and inertia of the absorber and the desorber on the transient period were considered. The investigation of the system performance under different heat inputs resulted in shorter transient period as the heat input is increased. On the other hand, when the inertia of the components was considered, the cycle took about 20 minutes before it reached the steady state operation, and that reflect the importance of taking the inertia of the components into consideration. The developed dynamic model is able to predict the transient performance of single-effect LiBr/Water absorption cooling machine which in turn helps in designing appropriate absorption systems for various applications while ensuring safe operation.

The performance of the solar absorption system was investigated under meteorological condition of Dhahran – Saudi Arabia for a representative day of summer. The result indicates that; an auxiliary heating system is needed to assist the solar system in order to empower the absorption cooling system by 14.67 kW required to cover a cooling load of 3 TR. The solar fraction ranges between 60 to 90% during noon times for collector areas between 25, and 35 m^2. Nevertheless, the evacuated tube collector is able to stand alone and satisfy the total required energy during the hour immediately after noon if the collector area is 40 m^2 (SF = 100%).

ملخص الرسالة

الاسم الكامل : حمزة كمال علي مختار

عنوان الرسالة : تحليل ثيرموديناميكي إنتقالي، لمولد في نظام تبريد إمتصاصي يعمل بالطاقة الشمسية مصمم لمناطق حارة و رطبة.

التخصص : الهندسة الميكانيكية

تاريخ الدرجة العلمية : ديسمبر, 2016 ، الموافق ربيع الأول 1438

يعرض هذا البحث تطوير نموذج ديناميكي لدورة تبريد إمتصاصي أحادية التأثير والتي توظف بروميد الليثيوم والماء كممتص ومبرد وذلك بإجراء تحليل ديناميكي حراري متغير مع الزمن. المشاكل المرتبطة بانبعاثات غاز ثاني أكسيد الكربون حفزت الباحثين في مجال الهندسة للتركيز على إيجاد بدائل لمصادر الطاقة التقليدية أو تطوير الموجود منها. بناء على ذلك، أجريت الكثير من الدراسات والتجارب على أنظمة التبريد الإمتصاصي لفهم أداءها الفعلي بدقة، وأدخلت الكثير من التعديلات بغرض تحسين وزيادة معامل الأداء لهذه الأنظمة. في هذا الصدد، حتى لو تم إفتراض أن الأثر التبريدي المطلوب كان ثابتا، وتم التحكم في كمية الطاقة الداخلة، سوف تكون هناك فترة عابرة تسبق فترة التشغيل في الحالة المستقرة للجهاز. طوال هذه المرحلة الغير مستقرة، معظم المعاملات تبقى تتذبذب ولا تستقر عند قيم معينة، والبعض منها قد يذهب بعيداً عن نطاقاتها المسموح بها بطريقة تؤثر على أداء الجهاز على نحو خطير. تعتبر هذه الظاهرة الحافز الرئيسي والشاغل الأساسي لهذه الدراسة. ويستند النموذج الديناميكي على قوانين إتزان الكتلة, الدفع, والطاقة مع الأخذ في الاعتبار الاستجابة الديناميكية للدورة ومع التركيز بصفة خاصة على أداء المولد الذي من المفترض أن يتم إمداده بالطاقة عن طريق نظام الطاقة الشمسية. وتُبين النتائج أن الدورة تستغرق في المتوسط حوالي 14 دقيقة قبل استقرار معظم المعاملات على قيمها التشغيلية المصممة لها، و تتلاشى الحدود الديناميكية في ما يسمى بالتشغيل المستقر. بعدها، تم التحقق من النموذج المبتكر مع نموذج ديناميكي متاح مسبقاً، فضلاً عن آخر يقوم على فرضية التشغيل في الحالة المستقرة. وتكشف المقارنة عن توافق مقبول بدرجة كبيرة مع كليهما. وقد كانت القيم الأولية المطبقة قد حسنت الى أبعد ما

يمكن لتجنب خطر التبلور طوال فترة التشغيل. وعلاوة على ذلك، تمت دراسات الآثار المترتبة من الحرارة المدخلة والكتلة الحرارية للممتص والمولد على الفترة التشغيلية العابرة. نتج عن التحقيق في أداء النظام تحت تأثير الكميات المختلفة للحرارة المدخلة ونتج عن فترات عابرة أقصر كلما زادت الحرارة المدخلة. من جهة أخرى، عند تم الأخذ في الاعتبار الكتلة الحرارية للمكونات، أخذت الدورة حوالي 20 دقيقة قبل أن يصل التشغيل للحالة المستقرة، وهذا يعكس أهمية أخذ الكتلة الحرارية للمكونات بعين الاعتبار عند نمذجة مثل هذه الأنظمة. النموذج الديناميكي المبتكر قادر على التنبؤ بالأداء الفعلي لماكينة التبريد الإمتصاصي أحادية التأثير التي تعمل بواسطة محلول بروميد الليثيوم والماء إلى حد بعيد، مما يساعد بدوره على تصميم أنظمة التبريد الإمتصاصي المناسبة لمختلف التطبيقات مع ضمان التشغيل الآمن.

بعد ذلك، تم التحقق من أداء نظام التبريد الامتصاصي بالطاقة الشمسية بناءً على معلومات الأرصاد الجوي لمدينة الظهران_ بالمملكة العربية السعودية ليوم ممثل لفصل الصيف. وتشير النتائج للحوجة إلى نظام تسخين مساعد بجانب النظام الشمسي بغرض إمداد نظام التبريد ب14.67 كيلو واط اللازمة لتغطية حمولة تبريد تساوي 3 طن تبريد. النسبة الشمسية تتراوح بين 60 إلى 90% خلال أوقات الظهيرة عندما تكون مساحة النظام الشمسي بين 25، و35 متراً مربعاً. غير أنّ النظام الشمسي يكون قادراً على توفير كامل الطاقة المطلوبة لوحده بين الساعة الثانية عشر والواحدة ظهراً إذا كانت مساحة المجمع الشمسي 40 متراً مربعاً (النسبة الشمسية = 100%).

شهادة ماجستير علوم

جامعة الملك فهد للبترول والمعادن

الظهران ، المملكة العربية السعودية

CHAPTER 1

INTRODUCTION

1.1 Background

1.1.1 About basic vapor sorption cycle

The principle of vapor sorption cycle is similar to that of vapor-compression cycle except the mechanism of compression process. In order to pressurize the vapor a compressor is used in the vapor compression cycle, which would consume much more mechanical or electrical power compared with a pump in a sorption system (Fig. 1.1). The basic idea of vapor sorption system is, low sorptivity at high temperature and vice versa. The main advantage of a vapor sorption system is the use of low grade energy to generate desired cooling effect.

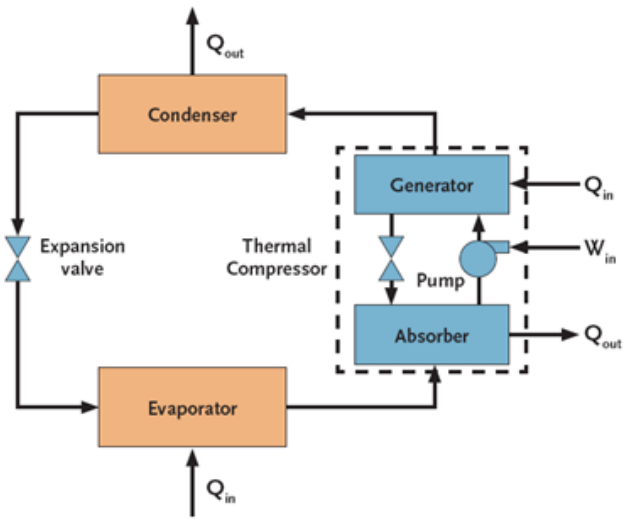

Figure 0.1: Basic absorption cycle.

In order to utilize the relatively high energy of the weak solution that goes back to the absorber; predominantly, a heat exchanger is introduced between the generator and the absorber to preheat the solution before it enters to the generator. This process decreases the amount of input heat required in the generator and subsequently increases the COP of the system (Equation 1.1) [1].

$$COP = \frac{Cooling\ Output}{Heat\ Input} \tag{1.1}$$

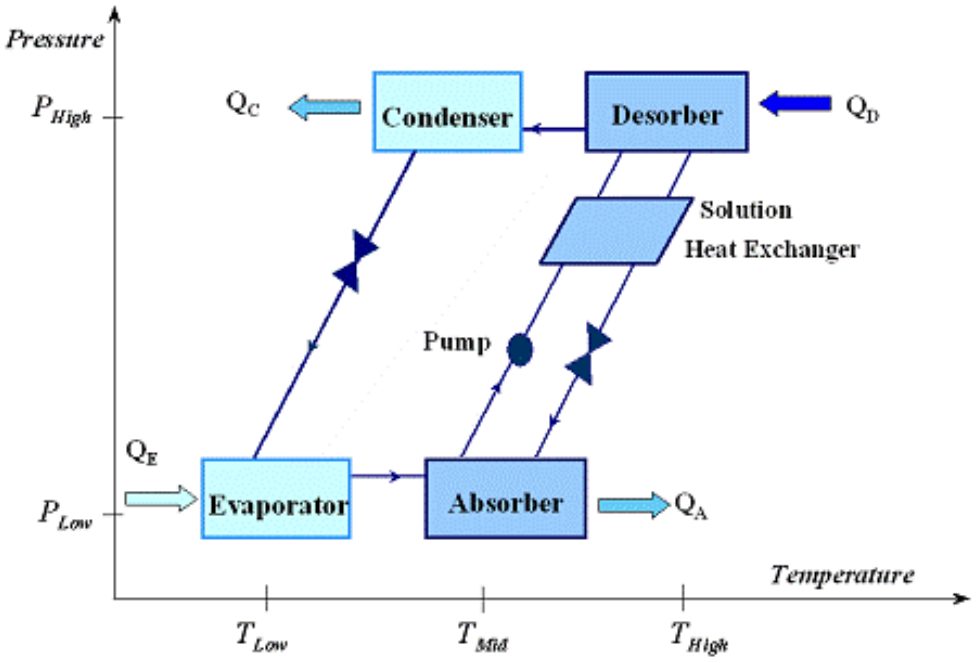

Figure 0.2: Introducing of a heat exchanger to the basic absorption cycle [1].

1.1.2 Different designs of absorption cooling cycle

1.1.2.1 Single-effect absorption cooling cycle

It is the simplest type among various absorption cycles [1]. It consists of the four main components, desorber, condenser, evaporator, and absorber (Fig. 1.1). A low temperature heat source is sufficient to run the cycle. It is suitable for small applications such as small office or single homes. A heat exchanger is introduced between the absorber and the generator seeking for reducing high irreversibility that takes place in the cycle (Fig. 1.2). This modification has considerable improvement in the coefficient-of-performance of the system. Other modifications might be applied on the basic cycle, but it has less effect on the COP (e.g. Refrigerant heat exchanger).

When aqueous ammonia is used as a working solution; a rectifier column and a Dephlegmator (Analyzer) _which is a heat exchanger_ are usually connected to generator in order to ensure that water vapor will not scape with the refrigerant into the condenser (Fig. 1.3).

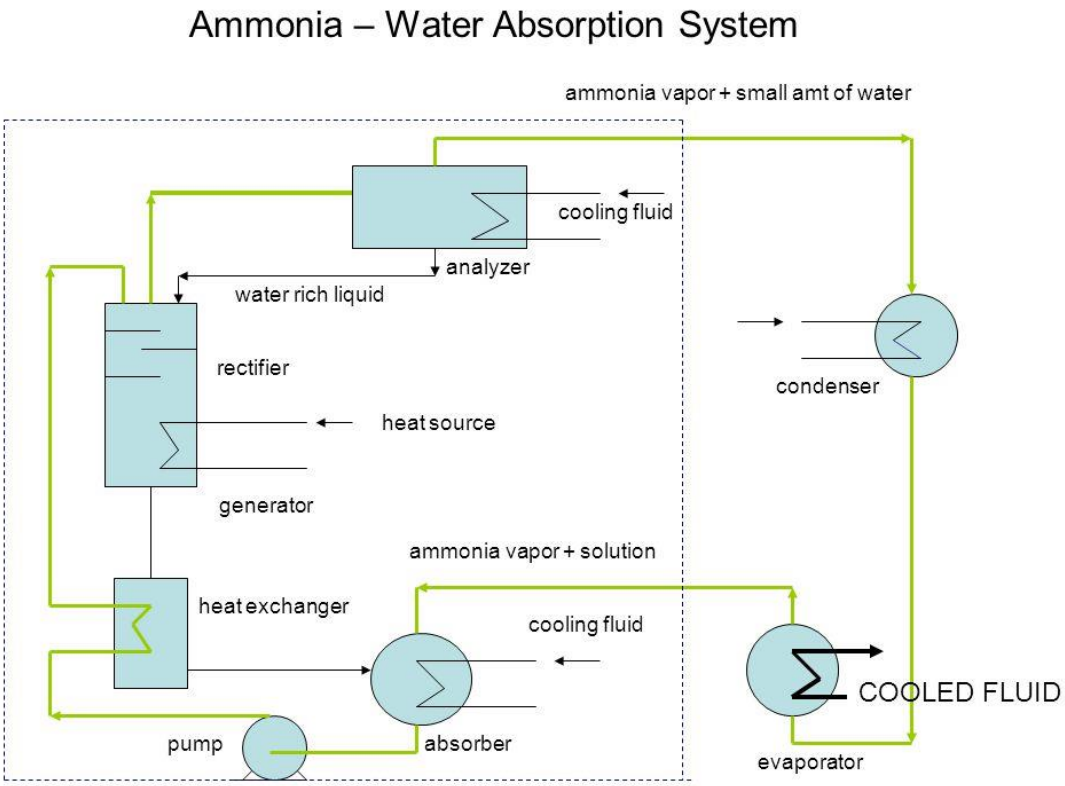

Figure 0.3: Single effect Aqua Ammonia absorption cycle [1].

1.1.2.2 Double-effect absorption cooling cycle

Looking for higher cycle efficiency, multi-effects absorption cycles are used (Figs. 1.4, 1.5, and 1.6). For example, in the double-effect lithium bromide water absorption cycle (Fig. 1.4) the heat contained in the regenerated vapor in stage one is utilized in the second stage desorber. The diluted solution in the first stage is directed to stage 2 to extract more refrigerant in the second generator. Hence, it is three pressure levels. Equation (1.2) [1] is used to estimate the COP of this cycle.

$$COP_{double\ effect} = COP_{single\ effect} + (COP_{single\ effect})^2 \quad (1.2)$$

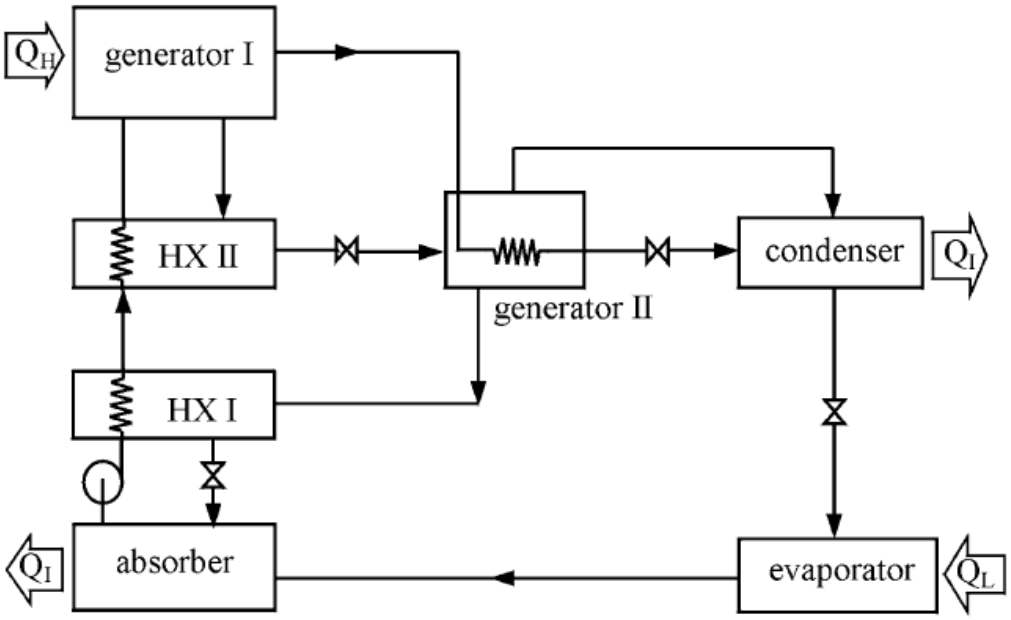

Figure 0.4: Double effect $LiBr/H_2O$ absorption cycle [1].

For ammonia water double-effect cycle (Fig. 1.5), only two pressure levels are established. An external heat source is applied to the generator of the second stage, whereas the absorbing heat released from the second absorber is recovered and utilized in the first generator, thus, this absorber should work at higher temperature to provide sufficient heat for the first stage generator.

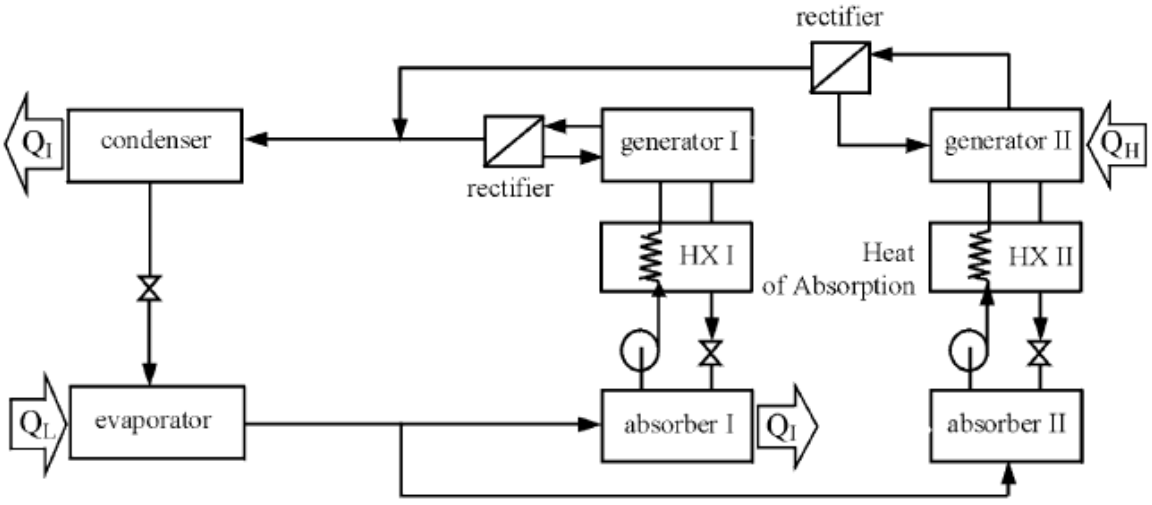

Figure 0.5: Double-effect Aqua Ammonia absorption cycle [1].

In the triple-effect absorption cycle there are four pressure levels. The condensation heat in the higher pressure stage is provided to the adjacent lower pressure stage to perform the refrigerant regeneration process.

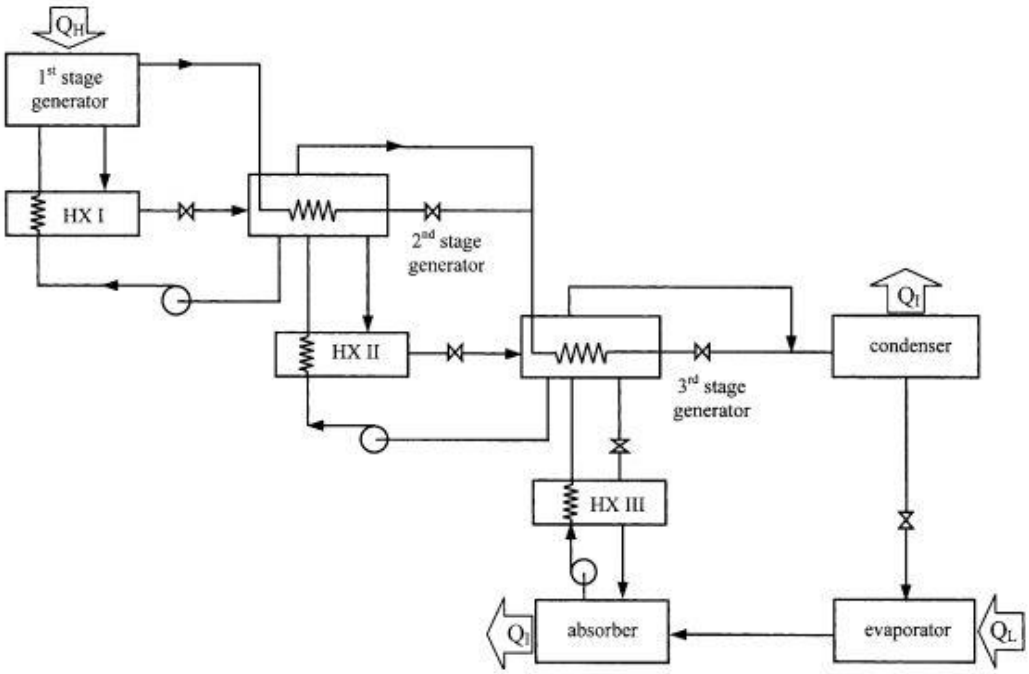

Figure 0.6: Triple-effect Aqua Ammonia absorption cycle [1].

1.1.2.3 Half-effect absorption cooling cycle

It is similar to the ammonia water double-effect cycle except in the process of providing the input heat. The low grade input heat is supplied into both desorbers, whereas, heat is rejected from both absorbers and this results in relatively less COP in comparison to double effect absorption cycle (Fig. 1.4).

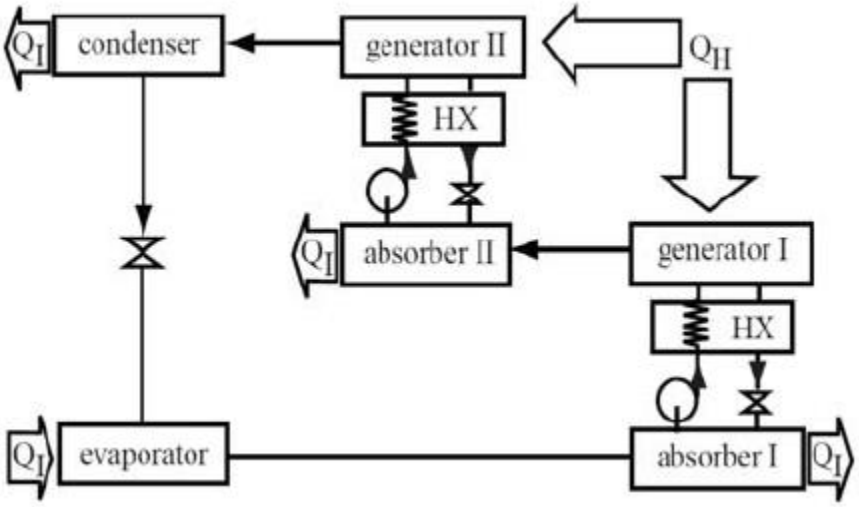

Figure 0.7: Half-effect absorption cycle [1].

1.1.2.4 GAX Absorption cooling cycle:

GAX is an abbreviation of generator-absorber-heat exchanger. The configuration comprises of two parallel single effect systems with introducing of a GAX to simplify it, and to rise its COP to be equal to that of double effect cycles, since the rejected heat from the absorber is recovered and used in the generator.

1.1.2.5 Absorption cooling cycle with an absorber heat-recovery

As the existing absorbent absorbs refrigerant that coming from the evaporator, an exothermic process takes place. This process dissipate a considerable amount of heat in the hot region of the absorber. In order to utilize this heat, a secondary fluid is circulated to the cooler region of the generator. Consequently, external input heat decreases and cycles' COP increases.

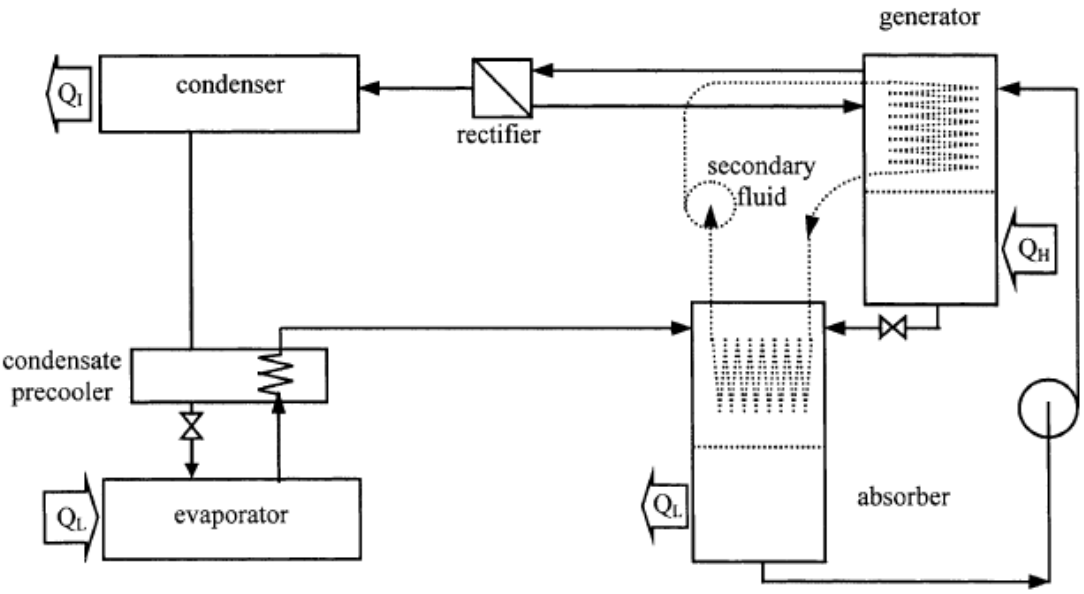

Figure 0.8: Absorption cooling cycle with an absorber heat-recovery [1].

1.1.2.6 Dual absorption cooling Cycle

It is like GAX and double-effect absorption cooling cycles. It involves two parallel single effect absorption cycle each with different working fluid. The principle of this type of cycles is to recover the heat released by the absorber and the condenser as well, which usually released to the atmosphere.

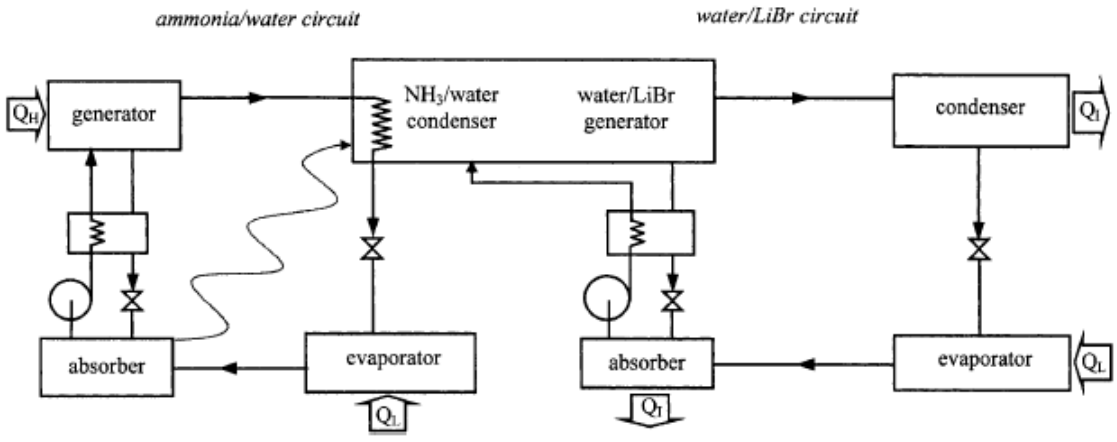

Figure 0.9: Dual absorption cooling cycle [1].

1.1.3 Working fluids

Absorption cycle employs sorbent in a liquid phase to perform the sorption process. On the contrary, adsorption cycle uses a solid material (e.g. Zeolite, Silica gel, and LiCl) to execute the sorption process. Table 1.1 lists some features of various sorption cycles.

Table 0.1: Characteristics of different sorption systems. "Regenerated from [2]".

Characteristic	**Water Chiller (Closed Thermodynamic Cycles)**						
Sorption material physical phase	Liquid				Solid		
Sorption material	H_2O	LiBr			Zeolite	Silica gel	LiCl
Refrigerant	NH_3	H_2O			H_2O	H_2O	H_2O
Cycle type	Single effect	Single effect	Double effect	Triple effect	Single effect	Single effect	Single effect
Range of COP	0.5-0.75	0.65-0.8	1.1-1.4	1.6-1.8	0.5-0.75	0.5-0.75	0.5-0.75
Range of driving Temp. °C [3]	70-100	70-100	140-180	200-250	65-90	65-90	65-90
Suitable solar technology	FPC, ETC, SAT	FPC, ETC	SAT	SAT	FPC, ETC	FPC, ETC	FPC, ETC

Refrigerant like ammonia (NH_3) is known to have high latent heat of evaporation and it is capable to meet subzero cooling demands. But at the same time NH_3 is highly corrosive and toxic [4]. Instead, water is used as a refrigerant in lithium bromide and water (LiBr-H_2O) absorption system but for cooling demand above zero degree. A brief comparison between the most common absorbent-refrigerant pairs is given in (table 1.2).

Table 0.2: Comparison between (H_2O-NH_3) & (LiBr-H_2O) absorbent-refrigerant pairs.

Solution type	**Advantages**	**Disadvantages**	**Considerations**
H_2O-NH_3	• Subzero demands. • High h_{fg}.	○ Corrosive. ○ Toxic.	• Rectifier column and Dephlegmator are needed
LiBr-H_2O	• Operates at low T_G. • Simpler. • Cheaper. • Quite operation.	○ Reduction in COP at high T_a. ○ Crystallization may occur.	• Certain limits of LiBr concentration to be maintained to avoid crystallization.

1.1.4 Solar cooling

Absorption cooling machines might be driven either electrically or thermally by using solar energy, exhaust gases from an engine, or from other heat resources, to produce quiet and reliable cooling. They do not use halogenated refrigerants which harm the atmosphere, and they can be utilized to diminish electrical peak demand that occurs in summer.

Currently, renewable energy is one of the most exploited engineering area of research that is attributable to the enduring need to improve the existing technologies, or even to develop new system that depends on such kind of energy. One of the most common application of renewable energy is *Solar Cooling*, which acts in producing cold from the solar energy [5]–[12].

1.1.4.1 Solar-driven absorption cooling system:

Among different solar air conditioning (AC) alternatives, solar-driven absorption cooling chiller is one of the commonly used systems. To far extend, it is similar to the classical vapor compression air conditioning system except in the compression mechanism where the electrical compressor is subrogated by absorber and generator driven by means of solar energy.

The beauty of solar driven sorption systems is that, the maximum demanded cooling effects synchronize with the abundance of the driving power (i.e. solar insolation in the summer months).

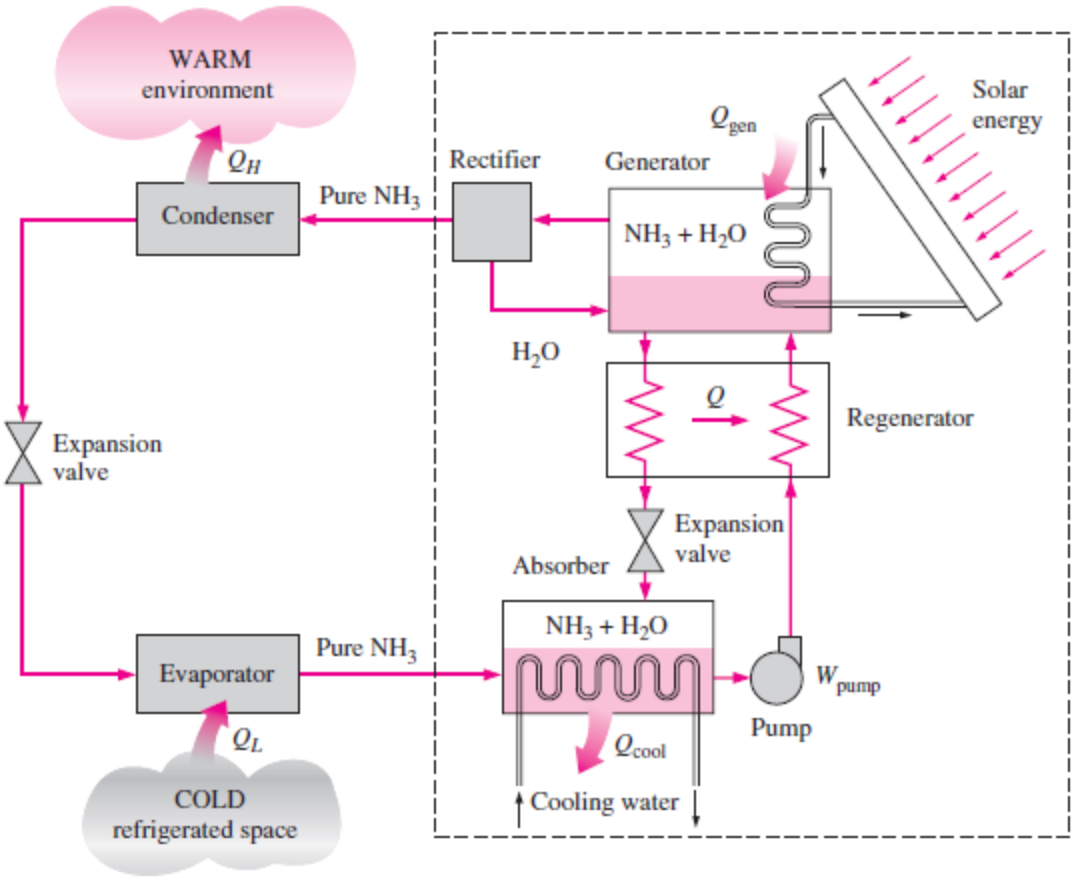

Figure 0.10: Solar absorption cooling system [13].

1.1.4.2 Solar collectors integrated with cooling absorption machines:

Allegedly, the different kinds of solar collectors can be applied for cooling purposes if the working temperature ranges of absorption chillers is specified. Normally, a heat source of the single effect LiBr/H_2O absorption chiller should be in the range of 75-100 °C to run the machine. Having a reasonably high efficiency at low working temperature, most likely flat plat solar collectors and single effect chillers are used together; while parabolic trough collectors and evacuated tube are applied to supply a high temperature heat source for double effect absorption chillers [14].

1.2 Motivation

Currently, renewable energy is one of the most exploited engineering area of research that is attributable to the enduring need to improve the existing technologies, or even to develop new system that depends on such kind of energy.

Owing to the progressive consumption of electricity which is predominantly generated from fossil fuel, the Kingdom of Saudi Arabia (KSA) is still be faced with high pollution. However, since KSA is located in the solar belt which has enormous potential to harness solar energy; the solar driven sorption systems are considered one of the most suitable systems for the Air-Conditioning (AC) and refrigerating purposes in the kingdom, and consequently, the issue of CO_2 emissions and the relevant problems (e.g. air pollution, global warming).

Technically, absorption systems show low coefficient of performance as compared to the vapor compression cycle. Accordingly, a lot of studies, experiments, and modifications have been conducted on the absorption systems to understand its actual performance minutely, improve it, increase its Coefficient of Performance (COP), optimize the cycle, and reduce its cost.

1.3 Thesis objective

The overall objective of this study is to carry out a transient thermodynamics analysis of solar-driven absorption cooling system to investigate the effect of varying solar input on the performance of the system. The specific objectives include:

- Develop a dynamic model for the absorption cooling system.
- Optimize the system performance to ensure safe operation without risk of crystallization.
- Investigate generator response and performance of the cycle under variable input solar energy.
- Assessment of using solar absorption cooling system in Dhahran – Saudi Arabia.

1.4 Research Methodology

The project work in this thesis, is mainly based on the following stages:

- **Background work and literature review:**

Comprehensive literature reviews over solar absorption cooling systems is presented in order to comprehend the scope of this project and retrieve the relevant data from the previously published studies.

- **Modelling work:**

The whole model will be based on mass, momentum, and energy balances and equations of state and heat transfer while taking into account the transient behavior of the system.

The mathematical modelling will be undertaken through the use of recognized and convenient software e.g. **E**ngineering **E**quation **S**olver (**EES**) in order to analyze the proposed system thermodynamically and assess its performance under different operating conditions.

1.5 THESIS OVERVIEW

This research encompasses five chapters followed by references, appendix, and vitae.

Chapter 1: **An Introduction** presents a background about the topic, work motivations, and specifies the general & specific objectives of this thesis and how the work will be executed.

Chapter 2: **Literature Review** summarizes the previous studies and conducted experiments related to the thesis scope, and points out the additional contribution of this study to the previous work.

Chapter 3: **Absorption System Model** introduces absorption systems, describes absorption cycle, puts assumptions for transient simulation, and elicits the mathematical formulations for every single components**.**

Chapter 4: **Results & Discussion** provides set of initial values, validates the developed model, shows the results extracted from the dynamic model, discusses it, , and discuss the crystallization phenomenon and explain how to avoid it.

Chapter 5: **Conclusion & Recommendations** pointing out the most important findings of this study, and suggest future recommendations.

CHAPTER 2

LITERATURE REVIEW

1.6 Previous studies on solar absorption cooling system

Jose A. Manrique [15] studied the probabilities to use solar energy to drive an ammonia-water system and to forecast its thermodynamics performance. The results indicate the feasibility to use solar irradiation to function as a heating source in an aqua ammonia absorption refrigeration system. A. Arsalis, and A. Alexandrou [16] prepared a design and model for solar heating/cooling system operated under lengthened hot climate condition. They studied the feasibility of utilizing solar energy to fulfill all thermal demand of residential building (e.g. heating/cooling load and domestic hot water). The maximum cooling load was set at 18.3 kW. Also, an auxiliary heating system is attached to a hot water storage unit and run during low solar irradiance periods. Additionally, they succeed to model the whole system and fulfilled a parametric study that helped in optimizing the performance of the economic system by making use of different design parameters. The optimization was done mainly to increase the solar fraction through manipulating with collector tilt angle on the monthly basis. The optimization is ended up with collector area of 70 m^2 and hot-water storage tank capacity of 7000 L. Afterward, regarding cost analysis a comparison with an electric heat pump has been made, where the overall annual cost is found to be $3,719. On the other hand, the precise analysis indicated that unless the cost of the solar collector is over $360/$m^2$; the SHC system would be preferable over electric heat pump systems. A. Acuna, *et al.* [17] found out the best generator temperatures which

produce maximum efficiency in absorption cooling systems employing. The absorption cycle runs with mixtures of (NH_3-$LiNO_3$) and (NH_3-NaSCN). Each system associated to a different type of solar collectors, which are: common and improved flat plate, evacuated tube, and compound parabolic trough collectors. The response of the cooling system overall efficiency is explicated. The results signify that both types of the flat plate collectors were not able to activate the system at ambient and evaporator temperatures of 40 and 0 °C respectively. Nonetheless, in case of evaporator temperature over 5 °C and surrounding at 30 °C; each working mixture would be activated despite of solar collector technology used to drive the system. The optimal coupling temperatures vary between 70 to 150 °C. The best configuration was which employing NH_3-$LiNO_3$ and driven by evacuated tube collector; which recorded 5 and 54% comparatively better than other configurations.

The limitation of this study has to do with the assumption that the system undergoes steady state condition, which is not true; and hence the resultant simulation is not entirely applicable. Z. Li, *et al.* [18] studied the performance of a double effect solar powered absorption cooling system using LiBr/H_2O, and involves air cooled condenser in subtropical city/climate. They primarily focused on the response of the system performance with the collector temperature in such regions. System's input parameters were: solar panels of 27 m^2 aperture area, 20° inclination angle toward south direction, evaporator settled at 5 °C, and 20 kW cooling capacity. A monthly basis climatological data was used in the simulation to develop a parametric model. Then, the average and hourly performance was analyzed based on the collector temperature. The optimum range of the collector inlet temperature to enhance system performance and minimize the probability of crystallization was found to be between 110–130 °C. The annual system performance inclusive overall

efficiency, cooling load per collector area and solar-fraction was presented. Moreover, the study investigated the behavior of the solar fraction and system efficiency with the heat exchanger effectiveness and pressure drop. They concluded with that, the effect of the two heat exchangers is almost identical as their effectiveness don't exceed o.8. Nevertheless, when it changes from 0.7 to 0.8 and the pressure drop is taken into account as 0.1 kPa; the relative alteration rate of average solar fraction of monthly typical day is 3.13% and 1.37%, whilst that of average overall efficiency is 3.13% and 1.12%. The authors tried to optimize the monthly average performance of double-effect absorption system by selecting the best tilt angle of the solar collectors. As expected, it is not fixed for each month. Thus, the optimum collector inlet temperature is not identical, and also differs according to existence of hot water storage unit or not. The later parameter had been investigated and the results demonstrate that, if the system involve a hot water storage unit; the optimal inlet temperature becomes higher. In contrast, the temperature of the absorber has insignificant influence on the compound parabolic concentrator optimal temperature. A. Ghafoor and A. Munir [19] carried out sensitivity analysis of solar-assisted cooling and heating system under Faisalabad (Pakistan) climatic conditions. A commercially available absorption chiller of 60 kW rated power was selected to satisfy the building's peak cooling demand. They used maximization of net positive value "NPV" to calculate its economic feasibility. Different economic parameters conditions were used to optimize the collector area and storage unit size. For instance, the effective interest rate affects the optimum collector area. Lower effective interest rate; larger collector area can be used, consequently producing higher solar fraction. Generally, they found that, the optimal collector area ranges between 0.26 m^2 and 0.36 m^2 associated with effective interest rates of 4.5% and 0.5% respectively.

The collector tilt angle was optimized and adopted at local latitude angle minus 11°. Eventually, their system needs financial incentives in order to be cost effective. However, saving potential of an enormous amount of conventional energy could be obtained as the solar fraction might reach 55 to 100% for cooling during summer, and 87 to 100% for heating during winter.

Lately, several mathematical models were evolved to design and to explore the performance of various LiBr-H_2O absorption systems. Micallef and Micallef [20] carried out a simple and clear linear mathematical model for an absorption cooling unit using either aqua-ammonia or lithium bromide water pairs. Through this simulation, and under different generator, condenser, and absorber temperatures; the system response was analyzed and presented. The mathematical model had been successfully verified by a numerical example in addition to an analogous simulation from *ASHRAE Fundamentals Handbook*, ASHRAE, Atlanta (2001). Mital *et al.* [21] used a similar model but solely for lithium bromide-water pair.

Regarding exergy analysis of absorption cycles; Zadeh, and Bozorgan [22] applied the first and second thermodynamics laws to determine the energy efficiency as well as exergetic efficiency of a single-effect absorption refrigeration system using water/lithium bromide pair. A code in EES software was developed to model the whole system and its components. The results indicated that the generator and absorber encompass the highest exergy destruction, and they have greater influence on the system efficiencies than the other components. The exergy destruction that occurs in the absorber and the generator increases with the temperature of the generator as the difference in concentration of strong and weak solutions increases. Accordingly, the generator could be classified as the most

important component of the absorption system, and especial considerations must be taken into account when it comes to design or selection of the generator. Another important outcome is that; the exergetic efficiency was found to be less than the energy efficiency due to the irreversibility within the system. Therefore, performing exergy analysis is recommended in designing an absorption system; because it is precisely identify real losses. Le Lostec, *et al*. [23] Tried to optimize the performance of a single-stage absorption chiller with an ammonia water solution considering steady-state conditions. Different parameters were assumed to be constant such as evaporator power, fluids temperatures in the entrances of the external heat exchangers, their effectiveness, and pump efficiency. The results show three optimal COP values that can exists by: minimizing the total irreversibility, minimizing the total thermal conductance, and maximizing the exergetic efficiency. Additionally, they showed that these values of COPs are less than the highest COP which corresponds to the internal and external temperatures convergence towards a mutual value. From exergy point of view, it is interesting to decrease the temperatures of the generator and the evaporator, and increase it in the absorber and the condenser. Nevertheless, these changes should be coupled by an essential rise in the total thermal conductance if a constant COP is desired to be preserved. They concluded that, to improve the COP and the overall exergy efficiency; an internal heat exchanger should be used.

Previously, most studies analyzed various solar absorption cooling cycles assuming that they run at steady-state conditions. But this is not the real behavior of the system, and due to the frequently changeable behavior of the system output, and the variable nature of the solar energy, the system performance is highly transient, and the assumption of steady state

condition is entirely wrong. This obligated the authors to come up with a realistic dynamic model that enable the prediction of the actual unsteady performance.

Recently, many researchers start taking into account the transient behavior of absorption refrigeration systems, and tried to come up with dynamic model that describe the real performance of these cycles. M. Ozgoren, *et al.* [24] investigated in hourly basis the performance of solar absorption cooling (SAC) system driven by means of evacuated-tube solar collector with aqua ammonia as a working solution. The transient behavior of the system characteristic is simulated based on climatological data of Adana province (Turkey). The maximum temperature which occurs on 29^{th} of July is considered in the performance evaluation. The fluctuations in values of several parameters like system efficiency, rates of heat transfer in both absorber and generator, and condenser capacity were recorded for different generator temperatures and cooling load. Subsequently, the minimum collector area was specified. The results pointed out that the SAC system is fairly suitable for residential and office buildings especially during daytime in that particular location. The best performance was recorded for generator temperature of 110 °C or higher. Predominantly, during the day the COP ranges between 0.243-0.454 and 1.243 to 1.454 for cooling and heating respectively. Solar collector area of 35.95 m^2 is required to satisfy 3.5 kW (1 TR) cooling load, while at noon time it goes down to 19.85 m^2. A. Iranmanesh, and M. Mehrabian [25] applied a lumped-parameter model to make a dynamic simulation. In order to avoid inaccuracy in some approximate relations; EES software was utilized to extract thermodynamic properties of LiBr-H_2O. Then a synchronization between MATLAB and EES software was made in order to solve the differential equations simultaneously. What was new is considering the impact of quality on the concentration of

solution at the outlets of absorber and generator. Moreover, a transient exergy analysis is carried out. The exergetic efficiency and COP declines with time, until reach the steady state values. The comparison indicates that the expectations of the transient simulation are in close matching with steady state results. Marc, *et al.* [26] implemented a clear dynamic model for 30 kW single effect LiBr/H_2O absorption machine harnessing solar energy by means of solar collector and operating without any heating or cooling backup systems. Thence, due to the frequently changeable nature of the solar insolation and the building loads; the system operates in transient state throughout the day. Here the circumstance obligated the authors to come up with a dynamic model that enable prediction of the actual performance. The model is based on equations of state, heat transfer equations, and mass and energy balances of each component. Posteriorly, an experiment setup was prepared to validate the temperatures and pressures of different components of the chiller. The validation results show consistency between the model and experiment results, particularly in outlet temperature of each component. Finally, the model is used to optimize the three source temperatures of the chiller "i.e. the generator inlet temperatures, the condenser, and the absorber", and hence obtaining better thermal COP according to different levels of cooling capacities. Other dynamic simulations have been developed. Weihua Cai, *et al*. [27] developed a dynamic-model of a single effect absorption refrigeration unit. The governing balances equations for the different system components were used to study the transient behavior of the cycle. Mixture equation of state was applied consistently to extract the thermodynamics properties. T. He, *et al.* [28] modeled and applied a new solar thermal absorption system in a standard office building in china with 50 TR cooling capacity, making use of locally made evacuated tube collectors. The system has storage unit for

heating, and likewise for cooling. TRNSYS software had been used for the modeling and optimization, then, their results have been validated via experimental tests. Thereafter, based on the simulation outcomes; system's economic performance and energy efficiency has been analyzed, result in annual average collectors efficiency equal to 37.6% with consequent solar fractions 0.76 and 0.38 in summer and winter respectively. F. Calise, *et al*. [29] simulated a model of solar-assisted cooling and heating systems in transient state considering three different configurations. In all cases, the SHC system consisted of evacuated tubes solar collectors, single stage lithium bromide-water absorption machine, and sometimes a boiler is used as an auxiliary system. TRNSYS software has been used to develop the simulation model, and an economic model was also developed. Moreover, a mixed heuristic deterministic optimization algorithm was executed to specify the set of the synthesis/design parameters that maximize the energy-efficiency of each configuration. The outcomes are heartening as for the energy saving potential. Conversely, the solar assisted cooling and heating systems seem to be ineffective from economical point of view; which is common drawback of most of renewable energy systems. A. Budania, *et al*. [30] came up with a model and simulation of a single-stage absorption chiller driven by solar energy using the transient simulation software 'TRNSYS'. Standard chiller performance data, along with collector efficiency parameters and storage tank loss coefficient evaluated from the conducted experiments were used to model the system. They ended up with a reality that the output of the system increases with the collector area, nonetheless, this increasing restricted by the capacity of the storage tank owing to the maximum water temperature allowed. Another observation had to do with the system controls; with an auxiliary heating; when storage tank capacity increased, the average output cooling

potential lessened because of lower water temperature. Conversely, without any auxiliary heating and depending on the collector area; an optimal size of the storage tank is attained. For 150 and 350 m^2 collector area; optimum size of storage tank was recorded as 2 and 5.8 m^3, respectively.

Several experiments were also conducted under different operating conditions to study and examine various models available in the literature. A. Syed, *et al*. [31] conducted an experimental test of a cooling system partially driven by solar energy for typical residences in Spain-Madrid during 2003 summer. The single-effect absorption chiller with a nominal capacity of 35 kW and employing ($LiBr/H_2O$) as a refrigerant-absorber pair had been driven by means of 49.9 m^2 flat plate collectors along with 2 m^3 stratified storage tank to store produced the hot water. At these particular locations the maximum solar insolation was 969 W/m^2 which produce corresponding cooling output of 5.13 kW whereas a 7.5 kW represented the maximum cooling capacity with 0.6 as maximum instantaneous COP, whilst 0.42 and 0.34 were recorded for daily and period averages. Other operational parameters especially the temperatures at different sections had been studied and clearly clarified. The study concludes with a predictable observation of that; the best system performance exist in hot and dry weather conditions. The resultant data might be considered as a benchmark to validate various mathematical models and to assess other analogous prototypes. V. Vazhappilly, *et al.* [32] designed, made and tested new prototype of an absorption refrigeration system utilizing exhaust-gases from an IC engine as a source of heat that required to evaporate the ammonia refrigerant. Thus, the generator system _the heating coil_ substituted by heat exchanger of frame plate type that has been precisely selected after specifying the heat released from the exhaust gases. M. Izquierdo, *et al.*[33]

designed and built an installation basically consists of flat-plate solar collectors of 48 m^2, hot water storage tank of 1500 liter, and combined single and double effect air cooled $LiBr/H_2O$ absorption chiller. The new prototype is able to operate interchangeably between single-effect unit (4.5 kW) and double-effect unit (7 kW). In case of single effect operation mode, the heat source is the solar energy. Whereas, an external heat source is probably required in double-effect operation mode. The evaporator is linked to a fan-coil unit located inside a laboratory analogous to typical Spanish households (80 m^2). The prototype was tested in August 2009 as a single-effect absorption system, and it had been able to satisfy about 65% of the seasonal cooling load, even though the system may meet the entire demand for few days. The other mode of the prototype can meet the demand too. However, it requires to warm up a thermal oil up to the operating temperature of the high pressure generator. Furthermore the system not only functions in single/double effect mode, but also it can run both modes simultaneously employing the mutual components of the two modes (e.g. absorber, condenser, evaporator, pumps and control equipment), but this configuration has not been tested in the experiment.

The above literature survey is summarized in a table form in Appendix.

1.7 Novelty

In this research a dynamic model will be developed for an absorption cooling system suggested to be fed by means of a solar collector coupled with a storage tank or a backup system to ensure a constant input power to the absorption system. The proposed dynamic model is able to simulate the transient state satisfactory; and supplement previous studies [27]–[30] which did not contain this level of details and complexity. Furthermore, this study draws the attention of importance of the initial state when it comes to transient analysis and how to optimize it in order to avoid crystallization. Finally, it addresses the effect of the heat input on the duration of the transient period.

CHAPTER 3

ABSORPTION SYSTEM MODEL

1.8 Introduction

The absorption cooling technology allows to produce the demanded cooling from solar energy or other low-grade energy sources in contrast to energy production systems that require relatively high grade energy sources. The operation of vapor absorption cycle is similar to that of vapor compression cycle except the mechanism of compression process. In absorption machine, a low grade heat is adequate to run the cycle. A low-grade heat can be obtained from the sun using solar collectors. Therefore, absorption systems are capable of being standalone systems when powered by solar energy.

Absorption cooling machines are most frequently used for air-conditioning and refrigeration applications. As indicated earlier, different pairs of absorbent/refrigerant are used in various absorption systems and applications. When absorption chillers are used in air conditioning systems the typical working solution is a lithium bromide-water solution. The refrigerant "water" is easily separated (desorbed) and absorbed from the absorbent "lithium bromide". This pair is usually used for cooling buildings, because it is capable to chill the refrigerant to the range of 4 $°C$ & 38 $°C$. Whilst in applications of food refrigeration (subzero demand); aqueous ammonia would customarily be used as it provide ideal range of temperature between - 51 $°C$ & 4 $°C$ which is suitable for this application [34].

Large scale lithium bromide-water absorption chillers (500 up to 1000 ton) are classically installed in power plants to provide enormous quantities of cold water for the purpose of cooling buildings or for applications of heat extraction in factories. In contrast, units of smaller capacity like (2-10 tons) are fit for air-conditioning of a small office or single home. The main focus of this study is small units.

For solar driven air-conditioning systems, the typical values of the COP are shown in Figure 3.1 for a given temperature of a heat source [35]. The COP is the ratio of the cooling effect produced by the machine relative to the input heat. It characterizes the performance of the cooling machine under different conditions, such as variation of heat input. Thus, based on the cooling demand or cooling load; the absorption cooling machine can be sized for a given desired location.

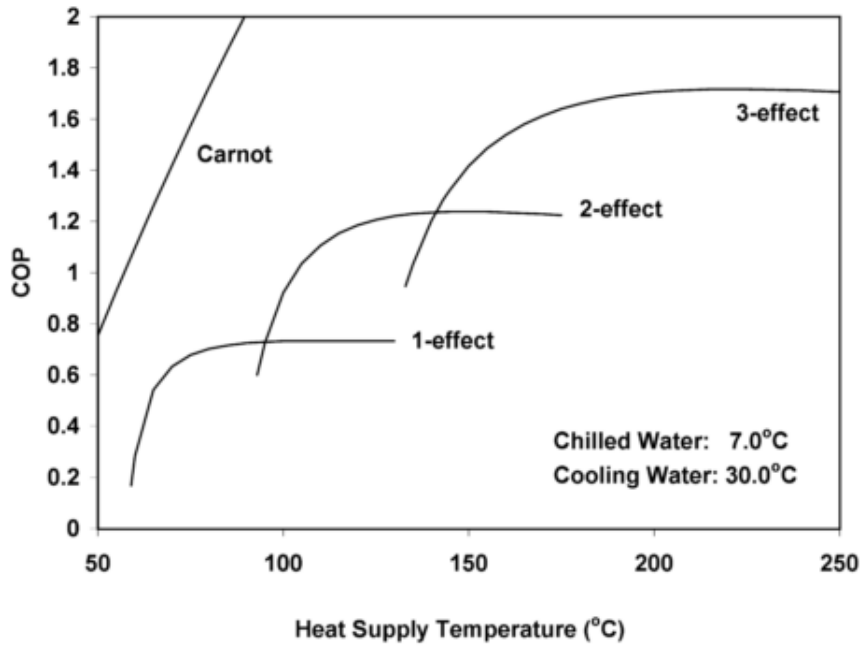

Figure 0.1: COP as Function of Input Heat for LiBr/Water Absorption systems [34].

In vapor absorption refrigeration cycle the COP is defined as the ratio of the cooling output to the heat input in the generator. Obviously, as more heat is supplied to the generator, the COP will increase as it shown in figure 3.1. Nonetheless, depending on the unit capacity; it might remain at constant level for a range of input power. Grossman study [35], reported that the COP keeps unchanged or might slightly decline, regardless of the added heat. This is apparently shown in Figure 3.1 for single, double, and triple effect absorption chillers. It is worth to be mentioned that, in that range the only way to increase the COP is by upgrading the absorption effect, on the other words, changing from a single to a double, or from double to triple effect cycle.

The COP of the vapor compression cycles which is the ratio of the cooling output to the input work ranges between 2 and 6.75. Yet, for similar cooling effect from both cycles, the cost of the required energy should to be taken into account since the input work is extracted from a high-grade heat source in the vapor compression cycle.

1.9 Absorption Cycle Description

A single effect absorption cycle is basically consist of four components, namely, absorber, desorber "or generator", condenser, and evaporator. The cycle is divided into a low pressure side and a high pressure side. The latter involves the generator and the condenser, while the low pressure side encompasses the absorber and the evaporator. The transition from the high pressure side to low pressure side occurs through two expansion valves, one for the refrigerant and the other for the solution, whereas, there is a pump to rise the cycle pressure. Usually, the pump discharges the solution at about ten times the lower pressures, nevertheless, it consumes less power than that required to drive the compressor in vapor-compression cycle. Notably, both low and high pressures in the absorption cycles are below the atmospheric pressure and the reason behind this is to ease the process of desorbing the refrigerant in the desorber as the refrigerant will boil off at moderate temperatures. In addition, the low pressure in the evaporator improves the evaporation process and increases the cooling output. The detailed understudy circuit diagram of a single-effect absorption cooling cycle that employs Lithium Bromide/Water pair is shown in figure 3.2.

In this cycle, the weak working solution (i.e. dilute $LiBr/H_2O$) is persistently pumped out the absorber to the generator. At the generator, the solution is heated up until the water vapor vaporizes and scape of to the condenser, leaving behind it the concentrated or strong solution which is combined again with the weak solution and then send it back to the absorber passing through an expansion valve to reduce the pressure to the low pressure of the cycle. Thereafter, the refrigerant "water vapor" gets cooled in the condenser by means of cooling water from an external loop. In order to reduce the pressure to the evaporator

pressure; the condensation falls down to the refrigerant expansion valve which comprised of small orifices. Now, the refrigerant has low pressure and temperature in the evaporator in which water gets chilled to be used for air-conditioning or refrigeration purposes. As the absorbent (LiBr) exists in the absorber has high absorptivity; it absorbs the water vapor from the evaporator and complete the cycle. Here it is worth to mention that the absorbent absorptivity increases as the temperature gets lessened. Accordingly, efficient cooling treatment should be carried out in absorber. The mathematical formulations used to develop the code that describes the aforementioned process but in the transient state are written and explained in Section 3.4. The program developed in this thesis is able to simulate single-effect LiBr/H_2O absorption cycles in unsteady state.

.

1.10 Assumptions for transient state model

The accurate prediction of the actual performance of the absorption machine is difficult. Thus, some reasonable assumptions are proposed to facilitate developing a good model.

- Lithium Bromide/Water solution is homogeneous across the cycle.
- Heat losses from/to all major components are negligible.
- The thermal inertia of the components is neglected in the first part of the thesis, however, as in real life it will be considered in the second part of the thesis.
- Constant weak and strong solution flow rates and heat exchanger effectiveness.
- Heat rate added to the generator and extracted from the absorber are constant.
- The lower pressure is fixed at specific value to prevent subzero temperatures (using adjustable orifices).
- Refrigerant exits from the condenser at saturation liquid state, and exits from the evaporator at saturation vapor state.
- Refrigerant exits from the generator has a temperature equal to that of strong solution at the exit of the desorber.
- The fluid properties at the exit of all major components is similar to the properties inside corresponding component.
- Neglecting masses of fluid in the condenser, evaporator, and expansion valves.
- The structures of the components are assumed to be at thermal equilibrium with the solution, then its mass and its thermal capacity can be composed with that of the solution and the structure itself

1.11 Mathematical formulation

This section represents the mathematical formulation for the components of the single effect absorption cycle which is shown in Figure 3.2. The appropriate mass and energy balance equations are used to model the transient behavior of the cycle. The system was dissected into major components (e.g. Desorber, Condenser, Evaporator, and Absorber), and secondary components (e.g. Expansion Valves, Pump, Heat Exchanger). Afterwards, each component was elucidated separately. Eventually, all balances equations were imported in EES software package to build a code that is capable to predict the dynamic response of the cycle.

The dynamic analysis is governed by the following conservation and balance equations:

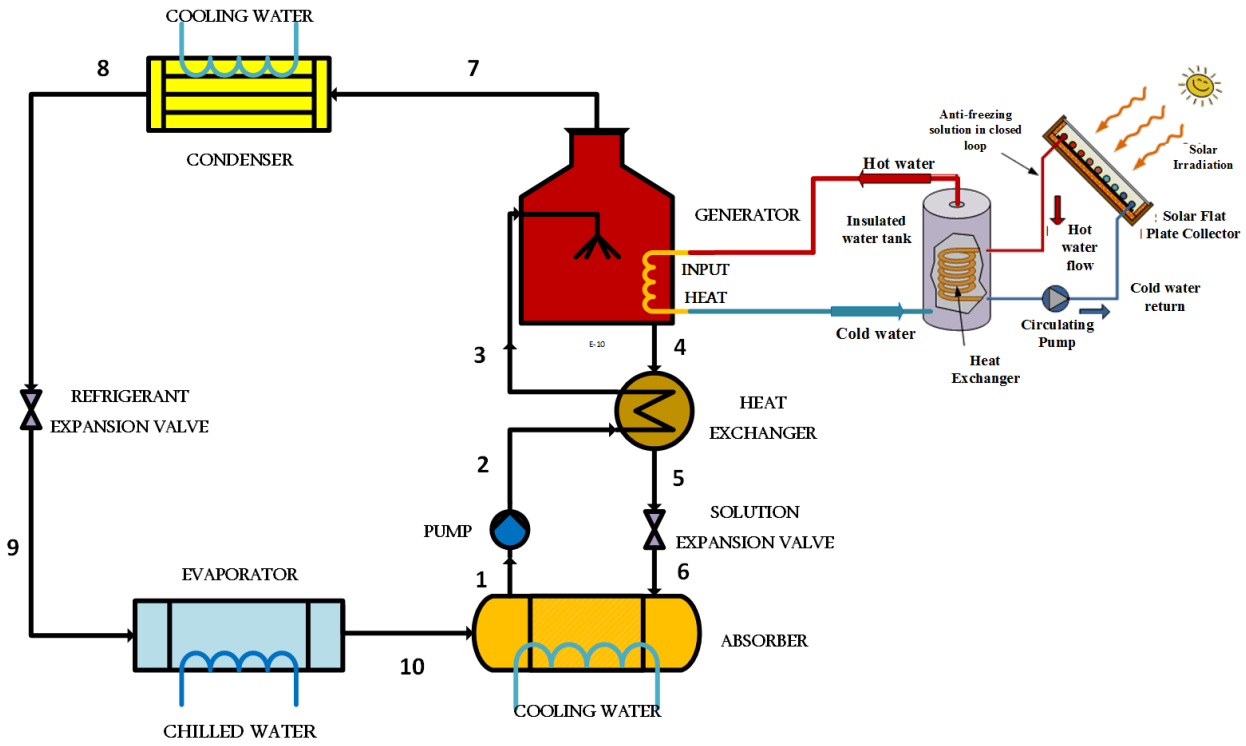

Figure 0.2: Solar absorption cycle under study.

1.11.1 Generator (Desorber)

The generator or the desorber is just like a boiler. The working solution inside it will heat up through a tube contains hot water comes from a storage tank or a solar collector directly. In various applications, the hot water or steam might be provided via other sources “e.g. hot exhaust gases from a plant”.

In figure 3.2, the weak solution that flows into the generator “state 3” mixes with the existing solution in the generator. Once it reaches the boiling-point, which is adapted at a specific operating pressure and temperature, the mixture will release water in a vapor phase at state 7. The released water vapor will flow towards the colder side of the condenser directly. Part of the strong solution will flow back to absorber “state 4” passing through the heat exchanger and the solution expansion valve as well, and the rest will remain inside the desorber.

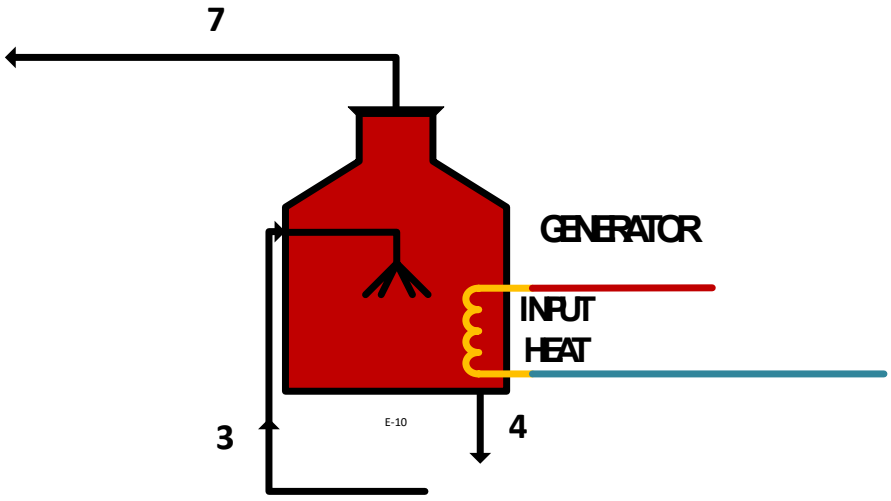

Figure 0.3: Desorber.

Performing mass, concentration and energy balances on the desorber results in the following:

Mass balance:

$$\frac{dM_G}{dt} = \dot{m}_3 - \dot{m}_4 - \dot{m}_7 \tag{3.1}$$

$$M_G = M_{G_i} + \int_{t_i}^{t_f} \frac{dM_G}{dt} \tag{3.2}$$

Concentration balance:

$$\frac{d(M_G.X_G)}{dt} = (\dot{m}_3.X_3) - (\dot{m}_4.X_4) \tag{3.3}$$

$$\frac{d(M_G.X_G)}{dt} = M_G\frac{d(X_G)}{dt} + X_G\frac{d(M_G)}{dt}$$

$$X_G = X_{G_i} + \int_{t_i}^{t_f} \frac{dX_G}{dt} \tag{3.4}$$

Energy balance:

$$\frac{dU_G}{dt} = \dot{m}_3.h_3 - \dot{m}_4.h_4 - \dot{m}_7.h_7 + Q_g - Q_{losses} \tag{3.5}$$

$$\frac{d(M_G.u_G)}{dt} = M_G\frac{d(u_G)}{dt} + u_G\frac{d(M_G)}{dt}$$

$$U_G = U_{G_i} + \int_{t_i}^{t_f} \frac{dU_G}{dt} \tag{3.6}$$

Losses:

$$Q_{losses} = (AU)_G(T_{solution} - T_{ambient}) \tag{3.7}$$

According to the second assumption above, $Q_{losses} = 0$.

1.11.2 Condenser

Figure 3.4 shows the condenser, where incoming water vapor from the generator “state 7” changes phase from vapor to a liquid form “state 8” as it gets cooled in the high pressure side of the condenser. This phase change process encourages the vapor flow from the hot region to the cold region, or explicitly, from the desorber into the condenser. The condenser comprises of a bundle of pipes or tubes in which cooling water being supplied, while condensation occurs over the tubes as the cooling water absorbs the heat of evaporation from the vapor.

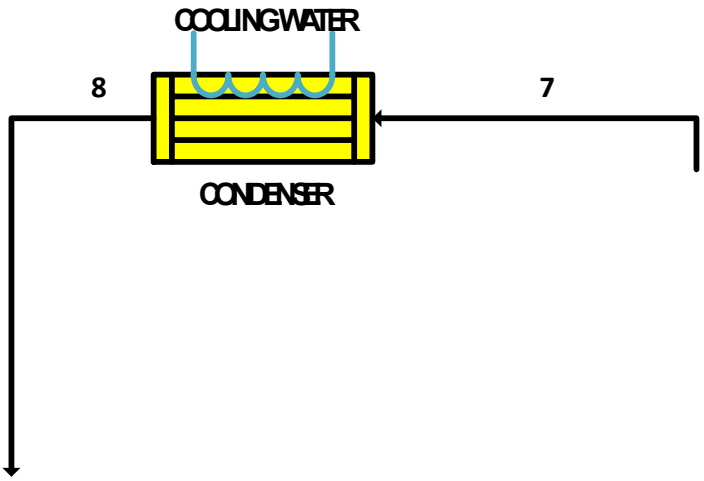

Figure 0.4: Condenser.

Performing mass and energy balances beside heat transfer equation on the condenser results in the following:

$$\frac{dM_C}{dt} = \dot{m}_7 - \dot{m}_8 = 0 \tag{3.8}$$

$$\frac{dU_C}{dt} = \dot{m}_7 . h_7 - \dot{m}_8 . h_8 - Q_C = 0 \quad or \quad Q_C = \dot{m}_7 . h_7 - \dot{m}_8 . h_8 \tag{3.9}$$

$$Q_C = (AU)_C (T_C - T_{cw}) \tag{3.10}$$

1.11.3 Refrigerant Expansion Valve

The pressure of the liquid refrigerant exit from the condenser "state 8" is reduced when it passes through this expansion valve, from the high pressure "condenser pressure" down to the low pressure of the cycle "evaporator pressure". The expansion valve in reality is small orifices through which the liquid refrigerant flows and flashes, resulting in decrease of both temperature and pressure "state 9", while the enthalpy remains constant (an adiabatic process, h8 = h9).

Performing mass and energy balances on the refrigerant expansion valve results in the following:

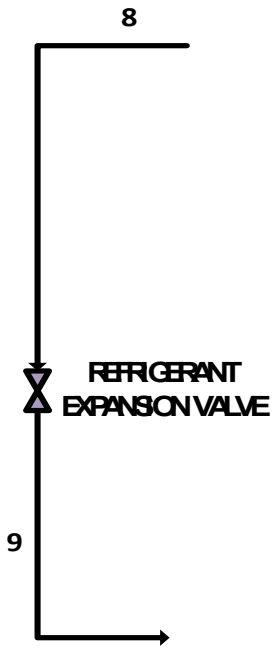

Figure 0.5: Refrigerant expansion valve.

$$\frac{dM_{REV}}{dt} = \dot{m}_8 - \dot{m}_9 = 0 \tag{3.11}$$

$$\frac{dU_{REV}}{dt} = \dot{m}_8 . h_8 - \dot{m}_9 . h_9 = 0 \tag{3.12}$$

1.11.4 Evaporator

Evaporator is the component of the absorption cycle in which the cooling effect of the cycle is produced, and it represents the low pressure region in the cycle. The condensed water exits from the condenser flows downward to the evaporator through the refrigerant expansion valve where it partially flashes. It reaches the evaporator at low temperature and pressure. Heat transfer process occurs between the water to be chilled and the refrigerant inside the evaporator. The refrigerant is assumed to entirely evaporate after this process, and then exits the evaporator as saturated vapor "state 10". As the liquid water is colder than the supplied water, the resulting is a chilled water produced in the tubes.

Performing mass and energy balances beside heat transfer equation on the evaporator shown in figure 3.6 results in the following:

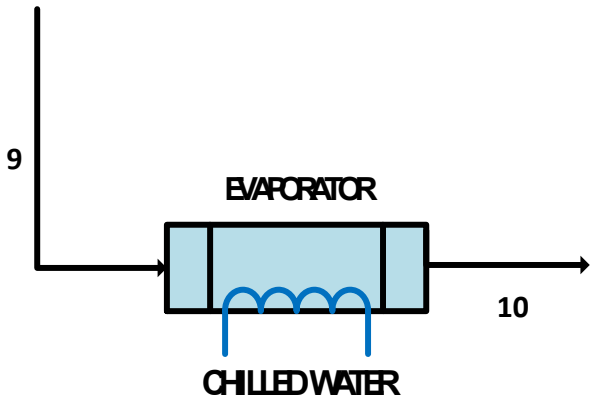

Figure 0.6: Evaporator.

$$\frac{dM_E}{dt} = \dot{m}_9 - \dot{m}_{10} = 0 \tag{3.13}$$

$$\frac{dU_E}{dt} = \dot{m}_9 . h_9 - \dot{m}_{10} . h_{10} - Q_E = 0 \tag{3.14}$$

$$or \quad Q_E = \dot{m}_9 . h_9 - \dot{m}_{10} . h_{10}$$

$$Q_E = (AU)_E (T_E - T_{ch}) \tag{3.15}$$

1.11.5 Absorber

The absorber is located in the lower pressure region at the absorption system, and its main function is to absorb the incoming refrigerant from the evaporator “state 10” and circulate it back to the generator “state 1”via the pump. There are two mass flow rates combined in the absorber; refrigerant vapor comes from the evaporator “state 10”, and the concentrated solution flows back from the generator through a line contains a solution expansion valve “state 6”. As the strong solution that flows back from the desorber reaches the absorber, the concentration and consequently the absorptivity of the existing solution intensifies. Hence, the water vapor produced in the evaporator absorbed into the absorber more and more, and the solution will be diluted before it being pumped.

Performing mass and energy balances beside heat transfer equation on the absorber shown in figure 3.7 results in the following:

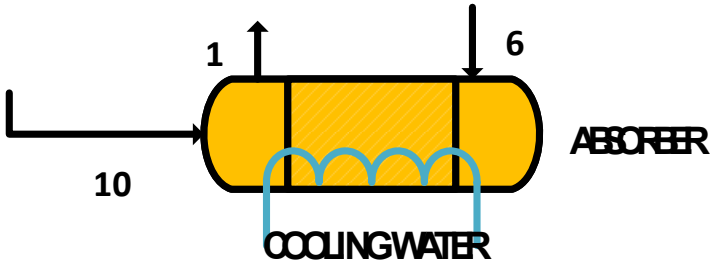

Figure 0.7: Absorber.

$$\frac{dM_A}{dt} = \dot{m}_{10} + \dot{m}_6 - \dot{m}_1 \tag{3.16}$$

$$M_A = M_{A_i} + \int_{t_i}^{t_f} \frac{dM_A}{dt} \tag{3.17}$$

$$\frac{d(M_A.X_A)}{dt} = (\dot{m}_6.X_6) - (\dot{m}_1.X_1) \tag{3.18}$$

$$\frac{d(M_A.X_A)}{dt} = M_A\frac{d(X_A)}{dt} + X_A\frac{d(M_A)}{dt}$$

$$X_A = X_{A_i} + \int_{t_i}^{t_f}\frac{dX_A}{dt} \tag{3.19}$$

$$\frac{dU_A}{dt} = \dot{m}_{10}.h_{10} + \dot{m}_6.h_6 - \dot{m}_1.h_1 - Q_A \tag{3.20}$$

$$\frac{d(M_A.u_A)}{dt} = M_A\frac{d(u_A)}{dt} + u_A\frac{d(M_A)}{dt}$$

$$U_A = U_{A_i} + \int_{t_i}^{t_f}\frac{dU_A}{dt} \tag{3.21}$$

1.11.6 Pump

The function of the pump is to rise the pressure of the solution exiting the absorber "state 1" and discharge it to the desorber.

Performing mass and energy balances on the pump results in the following:

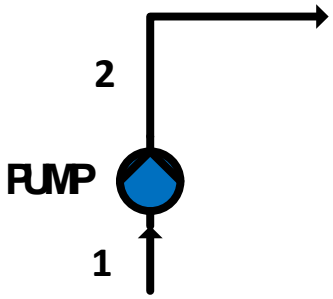

Figure 0.8: Pump.

$$\dot{m}_1 = \dot{m}_2 \tag{3.22}$$

$$W_P = \dot{m}_1(h_2 - h_1) \tag{3.23}$$

1.11.7 Solution Expansion Valve

The solution expansion valve is placed between the desorber and the absorber, and similar to the refrigerant expansion valve it is used to reduce the pressure of the concentrated solution before it enters the absorber “state 6”.

Performing mass and energy balances on the solution expansion valve results in the following:

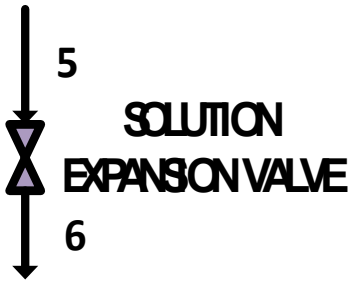

Figure 0.9: Solution expansion valve.

$$\frac{dM_{SEV}}{dt} = \dot{m}_5 - \dot{m}_6 = 0 \tag{3.24}$$

$$\frac{dU_{SEV}}{dt} = \dot{m}_5 . h_5 - \dot{m}_6 . h_6 = 0 \tag{3.25}$$

1.11.8 Heat Exchanger

One of the most useful modifications in the primary absorption cycle is introducing a heat exchanger between the absorber and the desorber. It is used to utilize the large thermal energy of the hot strong solution that coming out of the desorber “state 4” by transferring heat to the cool week solution pumped to the generator. Sometimes more than one heat exchanger are used depending on manufacturer specifications and recommendations. The

most important advantage of the heat exchanger is increasing the COP of the cycle by reducing the required input heat that used to desorb the water from the solution inside the generator. Additional advantage is reducing the cooling needs in the absorber which performs better at low temperatures.

Performing mass and energy balances beside heat transfer equation on the heat exchanger shown in figure 3.10 results in the following:

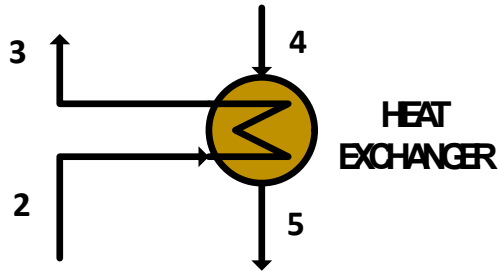

Figure 0.10: Heat exchanger.

$$\dot{m}_3 = \dot{m}_2 \quad \& \quad \dot{m}_5 = \dot{m}_4 \tag{3.26}$$

$$\dot{m}_2 . (h_3 - h_2) = \dot{m}_4 . (h_4 - h_5) \tag{3.27}$$

However, actually not all heat that released from the hot side of the solution is absorbed into the cool side of the heat exchanger. Hence, the heat exchanger effectiveness (ε) is given as:

$$\varepsilon = \frac{(T_4 - T_5)}{(T_4 - T_2)} \tag{3.28}$$

1.11.9 Whole cycle

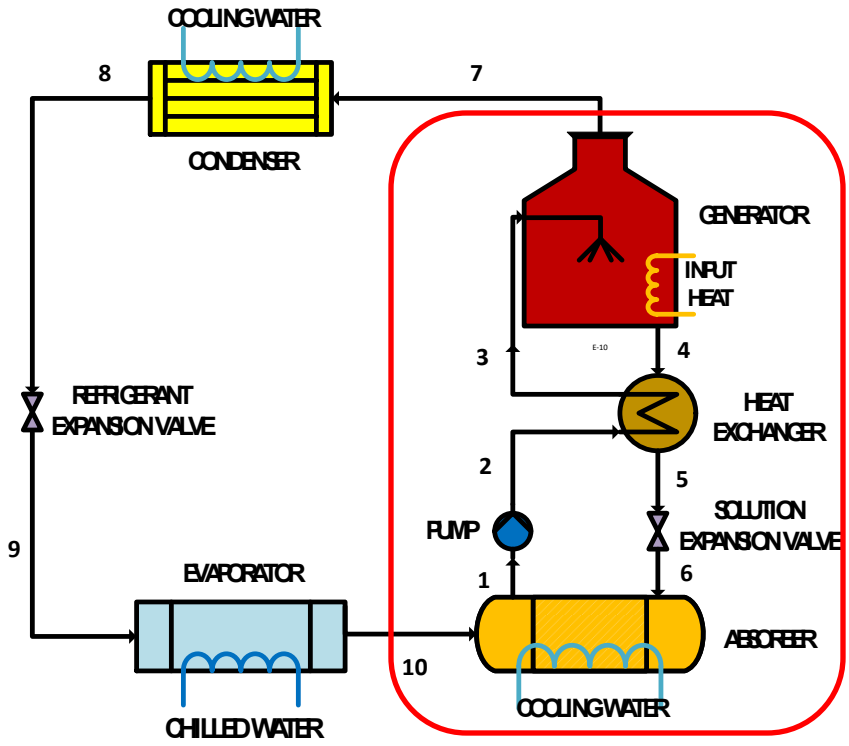

Figure 0.11: balance of the whole cycle.

Mass, concentration, and energy balances for the solution in the absorber and the desorber.

$$\frac{dM_G}{dt} + \frac{dM_A}{dt} = 0 \tag{3.29}$$

$$\frac{d(M_G * X_G)}{dt} + \frac{d(M_A * X_A)}{dt} = 0 \tag{3.30}$$

$$\frac{dU_G}{dt} + \frac{dU_A}{dt} = 0 \tag{3.31}$$

After completing the mathematical model by elucidating each component individually and the whole system, all balances equations were imported in EES software package to build a model that is capable to describe the dynamic response of the cycle. The software acts to solve equations simultaneously and conduct a lot of iterations until obtain converged solutions.

EES software package offers some functions that help in specifying the thermodynamic state of each of the points within the absorption cycle. Some of these functions are demonstrated in section 3.5. These functions play an essential role in developing the dynamic model.

1.12 Some of EES Functions used in developing the dynamic model:

- **T_LiBr : T = T_LiBr('SI' or 'Eng', P, X)**

Returns the saturation temperature over a lithium bromide/water solution as a function of pressure and concentration SI or British units.

- **P_LiBr : P = P_LiBr ('SI' or 'Eng', T, X)**

Returns the saturation pressure over a solution of lithium bromide and water as a function of temperature and concentration SI or British units.

- **V_LiBr : v = V_LiBr ('SI' or 'Eng', T, X)**

Returns the specific volume over a solution of lithium bromide and water as a function of temperature and concentration SI or British units.

- **H_LiBr : h = H_LiBr ('SI' or 'Eng', T, X)**

Returns the specific enthalpy over a solution of lithium bromide and water as a function of temperature and concentration SI or British units.

- **X_LiBr : x = X_LiBr ('SI' or 'Eng', T, P)**

Returns the concentration over a solution of lithium bromide and water as a function of temperature and pressure SI or British units.

- **Q_LiBr : Call Q_LiBr ('SI' or 'Eng', H, P, Z: Q, T, xL, hL, hV)**

Returns the quality, temperature, liquid composition, and liquid and vapor enthalpies of a lithium bromide-water two-phase mixture given the enthalpy pressure, and the solution composition in SI or British units.

- **Tcryst = LiBrSSCTCryst(X)**

Returns the crystallization temperature (in Celsius or Fahrenheit) corresponding to a given concentration.

The model is built by importing all equations extracted from the mathematical model into the software with an appropriate use of the EES functions. By introducing initial conditions and input values of some parameters the dynamic model is then able to describe the transient behavior of the system. Nonetheless, results of the developed model must be verified by comparing it with other valid model. Thereafter, the developed model can be optimized to ensure continuous safe operation. All those aspects are discussed in the next chapter.

CHAPTER 4

RESULTS AND DISCUSSION

1.13 Initial conditions

The case in this study is that, at t_o and before, the system operates at steady state. Thereafter, a higher solar radiation is considered which in turn means a higher heat input will be applied on the desorber and thus the cycle will undergo transient operation. A transient thermodynamic analysis is applied on the cycle to observe the response of the system to this change. Distinctly, the general trend of most internal parameters of absorption system such as (m_7, X_g, h_g, COP, Temperatures at different points, etc.) is that, they fluctuate at the commencement of the system operation after that change. Thereafter, most of them stabilize at certain values in what could be considered steady-state period. The initial values of some parameters in the initial steady state are listed in table 4.1.

The initial values in table 4.1 is similar to those initial value used in reference [25] in order to validate the results of the developed model in this study with the results of the dynamic model reported in reference [25].

It worth to mention that, when the inertias of the absorber are neglected the values of the heat capacity of the generator and the absorber are 25.2 and 29.5 kj/kg respectively. Whereas, when the inertias are taken into account the cumulated heat capacity of both are 58.5 kj/kg. (43% for the solution and 57% for the structure).

Table 0.1: Initial values of some parameters [25].

Parameter	Symbols	Initial value	unit
Initial mass in the generator	Mg_i	14	kg
Initial concentration in the generator	Xg_i	69	%
Initial enthalpy in the generator	hg_i	300	kj/kg
Initial mass in the absorber	Ma_i	15	kg
Initial concentration in the absorber	Xa_i	51	%
Initial enthalpy in the absorber	ha_i	35	kj/kg
Mass flow rate of solution exiting from absorber	m_1	0.05	kg/s
Mass flow rate of solution exiting from generator	m_4	0.0455	kg/s
Regenerated refrigerant	m_7	0.00445	kg/s
Effectiveness of the heat exchanger	ε	0.64	-
Pump work	Wp	0.000206	kW
Input heat to the generator	Qg	14.678	kW
Cumulated heat capacity of the generator [36]	$(M_s.C_{p_s} + M_{st}.C_{p_{st}})_G$	58.5	kJ/K
Cumulated heat capacity of the absorber [36]	$(M_s.C_{p_s} + M_{st}.C_{p_{st}})_A$	58.5	kJ/K

1.14 Validation

The model used in this study is validated against steady state model reported in reference [37], and the dynamic model developed by A. Iranmanesh et al. [25], for the same initial conditions and input parameters.

The comparison of results obtained by the current model with the ones reported in reference [37] & [25] are shown in tables 4.2 & 4.3. The comparison indicates a very good agreement with a maximum error of about 7%.

Table 0.2: Validation of the developed model vs steady state analysis [37].

	Q_a	Q_g	Q_c	Q_e	COP	P_{high}	P_{low}	X_4	X_1
Steady-state model	14.039	14.68	11.21	10.57	0.72	7.347	0.679	62.4	56.7
Current Model	14.04	14.68	11.95	11.3	0.77	6.857	0.68	63.16	57.03
Error Percentage % (Absolute values)	0.0071	0.014	6.573	6.9	6.9	6.669	0.147	1.218	0.582

Table 0.3: Validation of the developed model vs simulation results reported in [25].

	Q_a	Q_g	Q_c	Q_e	COP	P_{high}	P_{low}	X_4	X_1
Dynamic Model	13.792	14.77	11.23	10.59	0.717	7.35	0.67	62.23	56.82
Current Model	14.04	14.68	11.95	11.3	0.73	6.857	0.68	63.16	57.03
Error Percentage % (Absolute values)	1.76	0.63	6.0	6.7	6.9	7.19	1.47	1.47	0.36

1.15 Results and discussion

The results obtained based on the simulation of the absorption system will be presented and discussed in the following section:

1.15.1 Regenerated refrigerant (m_7):

The first set of results pertains to the rate of change of different parameters in the generator with time. The variation of refrigerant regeneration with time is presented in figure 4.1.

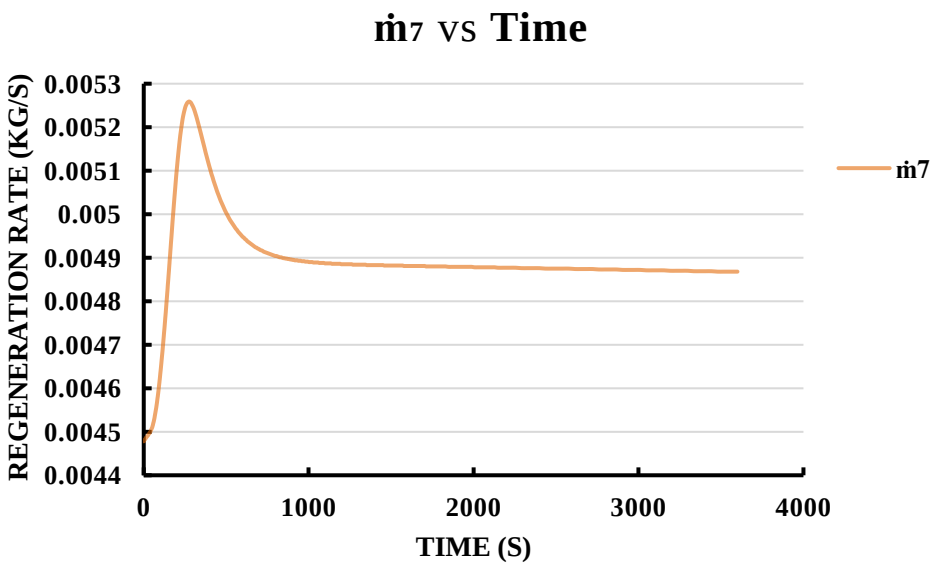

Figure 0.1: Refrigerant regeneration rate.

The figure indicates that, as the solution existed in the generator is assumed to be initially at relatively high temperature; refrigerant keeps regenerating from the solution as more heat being added. At the beginning, the regeneration grows up sharply because the pressure increases with adding more heat (fig 4.12). However, when the pressure start to decrease the orifices throttled more and limits the flow of refrigerant; thus, it declines until it nearly reaches a constant value of 0.0049 kg/s at steady state operation.

1.15.2 Mass of the solution in the generator and absorber (Mg & Ma):

The variation of the mass of the solution in the generator and absorber with time is shown in figure 4.2.

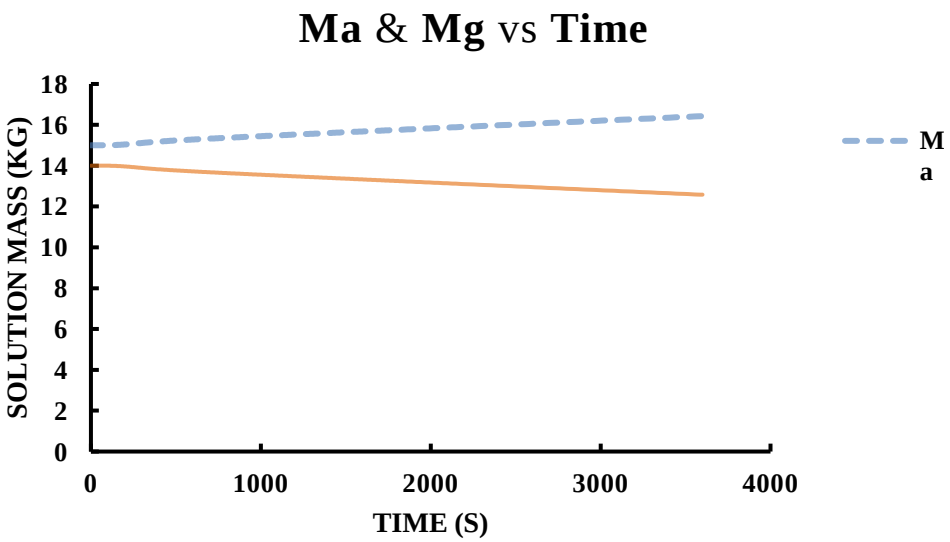

Figure 0.2: Solution mass in the absorber and the generator.

The results indicate that the mass of solution decreases in the generator, while it increases in the absorber; keeping the total mass of the solution constant. The mass of the solution inside the generator decreases mostly all the time because the water vapor generated in a rate higher than the constant difference between the mass flow rate of the weak solution that enters the generator and the mass flow rate of the strong solution that exits from the generator. However, the decreasing rate of the solution mass decreases with time and it should diminish to keep the mass of the solution inside the generator constant.

1.15.3 Concentration of the solution in the generator (Xg):

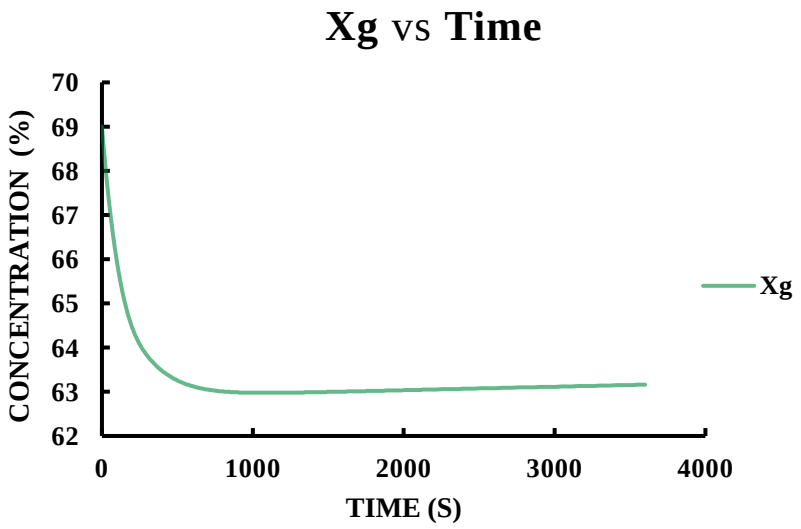

Figure 0.3: Concentration of the solution in the generator with time.

Figure 4.3 above shows the variation of concentration of the solution in the generator with time. A quick drop occurs from the initial concentration (i.e. 69% LiBr) to steady state value (approximately 63% LiBr) in an interval of approximately 480 seconds. The primary drop in concentration refers to the reality that at each moment a certain amount of weak solution enters and other of strong solution leaves, even though the regeneration is going on but the eventual consequence is decline in concentration. At steady-state operation a very small increase rate is observed in solution concentration due to the reduction in the total mass inside the generator beside the corresponding constant regeneration rate during this period.

1.15.4 Specific enthalpy of the solution in the generator (hg):

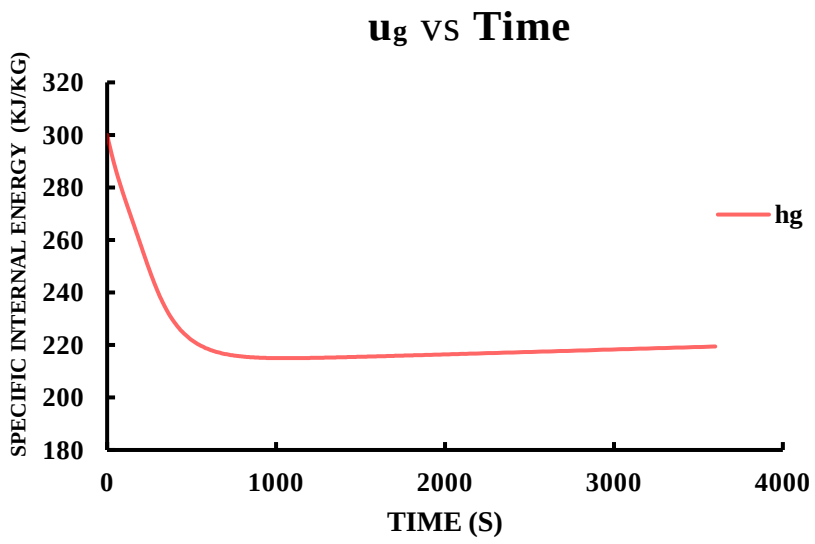

Figure 0.4: Specific internal energy in the generator with time.

The change of specific internal energy of the solution in the generator with time is shown in figure 4.4. The figure indicates a quick drop in the specific internal energy from the initial values (300 kJ/kg) to steady state values (about 220 kJ/kg) in an interval of approximately 480 seconds. The drop during the initial period of time refers to the high rate of refrigerant boil-off. An inconsiderable increase is observed in the specific internal energy during the steady-state operation because of continuous heat supply, in addition to the reduction in the total mass inside the generator.

1.15.5 Change of the solution mass in the generator with time:

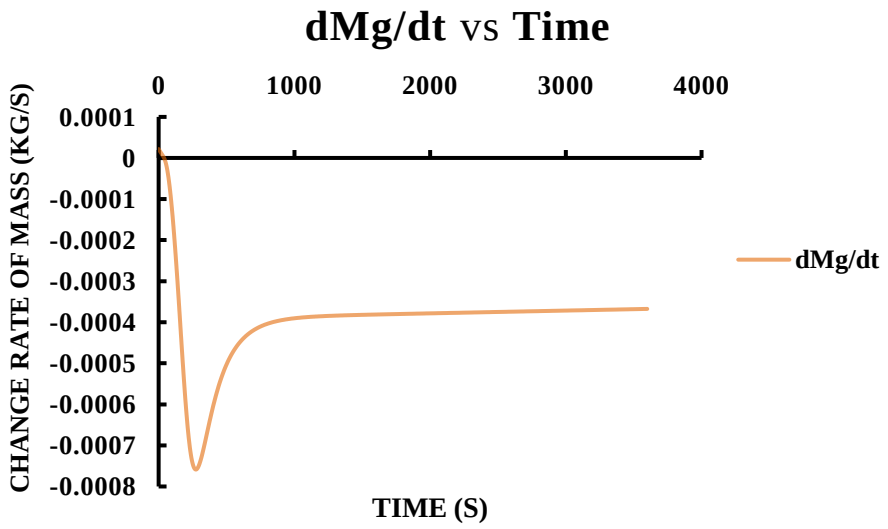

Figure 0.5: The rate of change of solution mass in the generator with time.

The rate of change of solution mass in the generator with time is shown in figure 4.5. This changing rate is substantially associated with the boil-off rate. It is negative nearly all the time; because the regeneration rate is always greater than the difference between the mass flow rate entering and exiting the generator. Initially it sharply decreases as the pressure increases (fig. 4.12), but when the pressure decreases the orifices chokes out and suppresses the flow of the refrigerant. Note that, figure 4.5 is a mirror image of figure 4.1 with subtracting the difference between the flow rates of the weak and strong solution.

1.15.6 Change rate of the solution concentration in the generator:

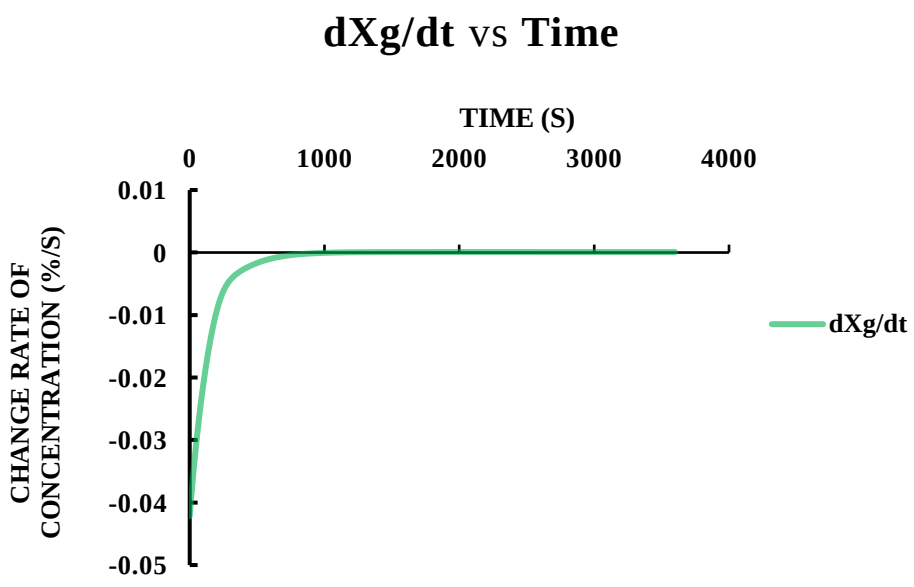

Figure 0.6: Change rate of solution concentration in the generator with time.

As it can be clearly seen in figure 4.3, the concentration of the solution inside the generator falls until it settle in steady state values, or in other words, the change rate of concentration approaches zero as it happens in figures 4.6. The primary drop in concentration refers to the reality that at each moment a certain amount of weak solution enters and other of strong solution leaves, even though the regeneration is going on but the eventual consequence is decline in concentration. At steady-state operation a very small increase rate is observed in solution concentration due to the reduction in the total mass inside the generator beside the corresponding constant regeneration rate during this period.

1.15.7 Change rate of the solution specific enthalpy in the desorber:

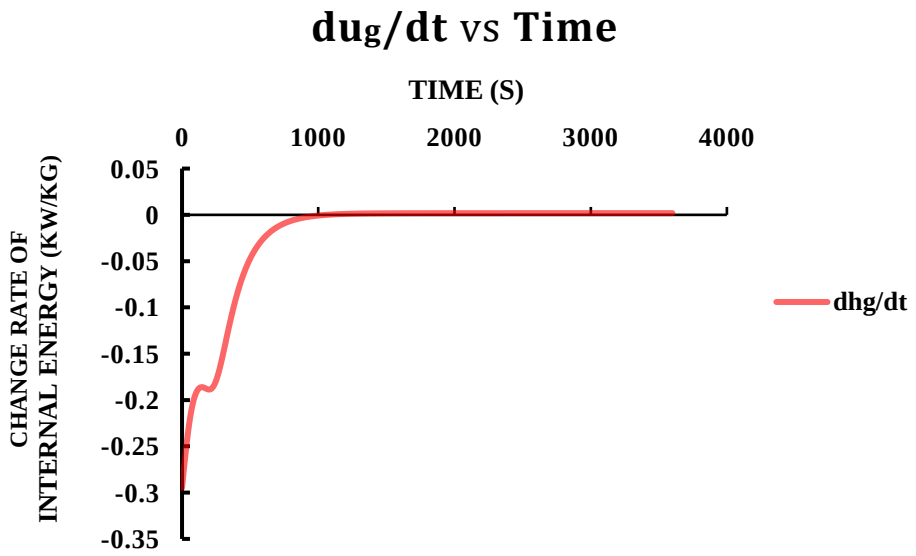

Figure 0.7: Change rate of solution specific internal energy in the desorber with time.

As it can be clearly seen in figure 4.4, the specific enthalpy of the solution inside the generator falls until it settle in steady state values, or in other words, the change rate of specific enthalpy approaches zero as it happens in figures 4.7. The primary drop in specific enthalpy refers to the reality that at each moment a certain amount of relatively low temperature solution enters and other of high temperature solution leaves, even though the heat is added continuously; but the eventual consequence is decline in specific enthalpy. At steady-state operation a very small increase rate is observed in the specific enthalpy of the solution due to the reduction in the total mass inside the generator beside the corresponding constant heat supply during this period.

1.15.8 Change rate of LiBr mass in the generator:

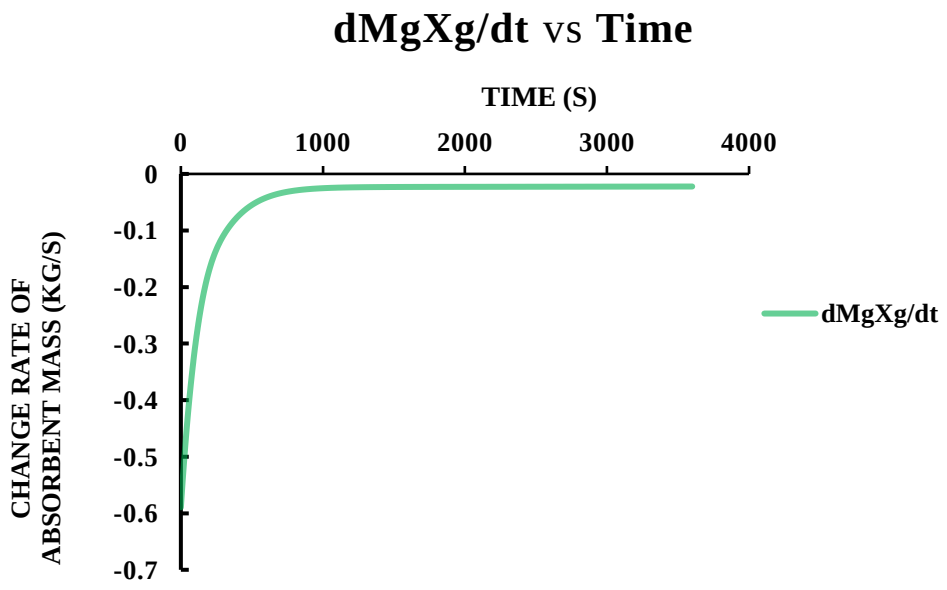

Figure 0.8: Change rate of absorbent mass in the generator with time.

The term “concentration” is an expression that reflects the amount of the lithium bromide in the solution. Likewise, the absorbent change rate “figure 4.8” is nearly typical to the change rate of concentration figure 4.6. It reduces until stabilizes at approximately zero at steady state phase.

1.15.9 Change rate of internal energy inside the generator:

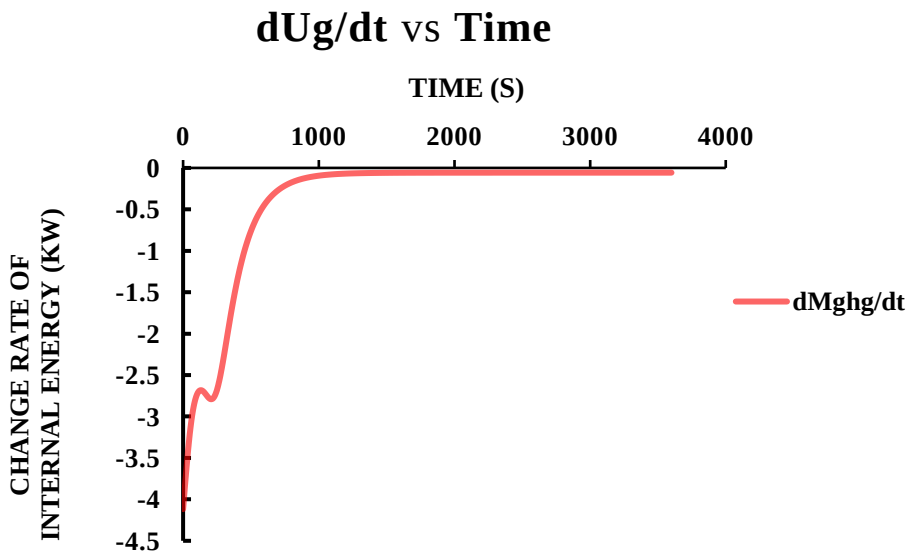

Figure 0.9: Internal energy change rate inside the generator.

The term in "y" axis represents the change rate of generator energy. It composes of two terms of four parameters

$$\frac{d(M_G.u_G)}{dt} = \left(M_G.\frac{d(u_G)}{dt}\right) + \left(u_G.\frac{d(m_G)}{dt}\right) \quad (4.1)$$

Nevertheless, the first term has the crucial effect, consequently, figure 4.9 is asymptotic to figure 4.7 with some scale up because it multiplied by solution mass at each moment of time, in addition to the effect of adding the second term.

1.15.10 Solution concentration in both sides of the heat exchanger:

The second set of results pertains to the solution concentration in the heat exchanger between the desorber and the absorber of the absorption cycle in figure 3.2. The change of solution concentration for the weak and strong solutions with time in the heat exchanger is shown in figure 4.10.

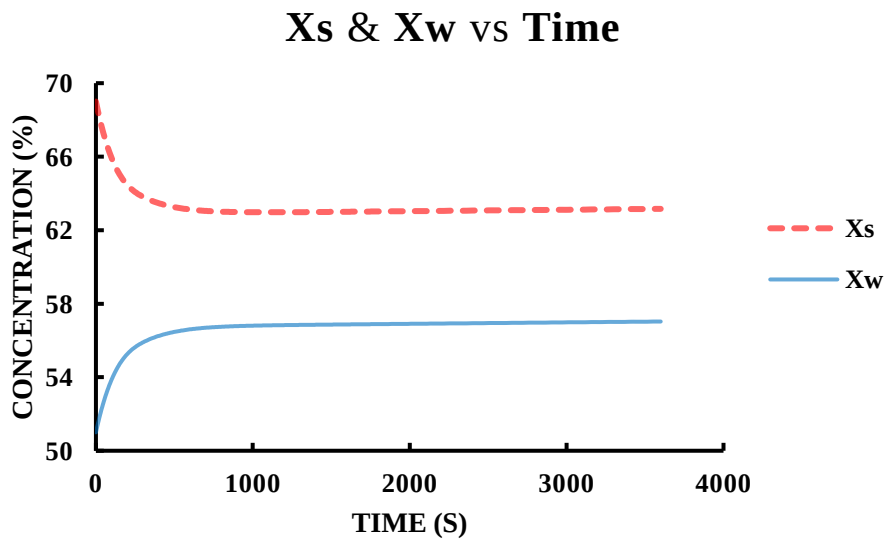

Figure 0.10: Change of concentration of the weak & strong solutions with time.

According to the assumption which state that; fluid properties at the exit of all major components is similar to the properties inside corresponding component; the concentration of the strong solution side of the heat exchanger has the same declining trend as the concentration of the solution in the generator. Also the concentration of the solution is the same along the strong solution side ($X_4 = X_5 = X_6$), and similarly for the weak solution line ($X_1 = X_2 = X_3$).

1.15.11 Coefficient of Performance “COP”:

The third set of results pertains to the change of coefficient of performance and the pressure of the cycle with time. The change of coefficient of performance of the cycle with time is shown in figure 4.11.

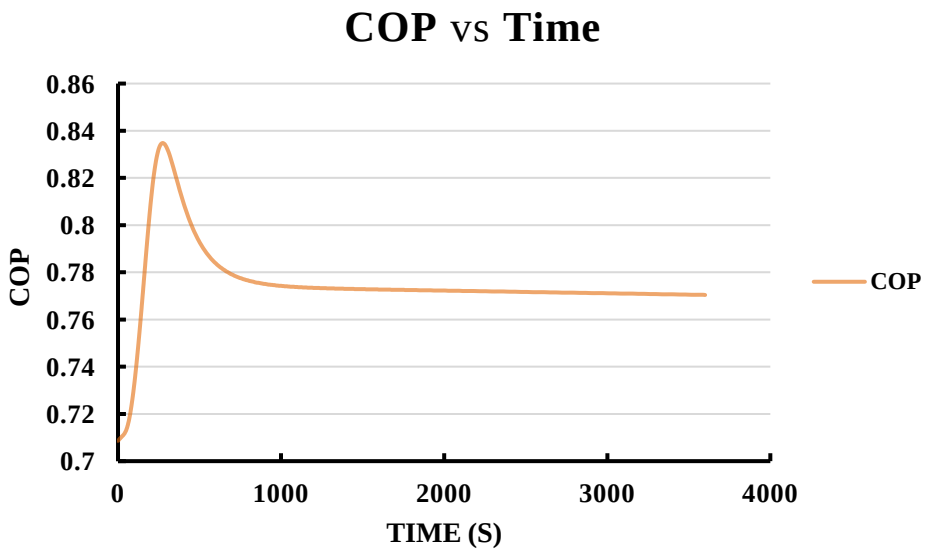

Figure 0.11: Coefficient of performance of the cycle (COP).

In absorption cooling systems the Coefficient of Performance (COP) is defined as the ratio between the cooling effect produced in the evaporator divided by the heat input in the generator. The heat input to the generator that is provided by a solar system is assumed to be constant. Hence, the coefficient of performance (COP) depends only on the cooling effect of the cycle, which substantially depends on the amount of refrigerant regenerated in the desorber because the evaporator pressure is fixed. Accordingly, the curve of the COP (figure 4.11) takes the same shape as the amount of regenerated refrigerant curve (figure 4.1).

1.15.12 Pressures:

The high pressure of the cycle change with time as shown in figure 4.12

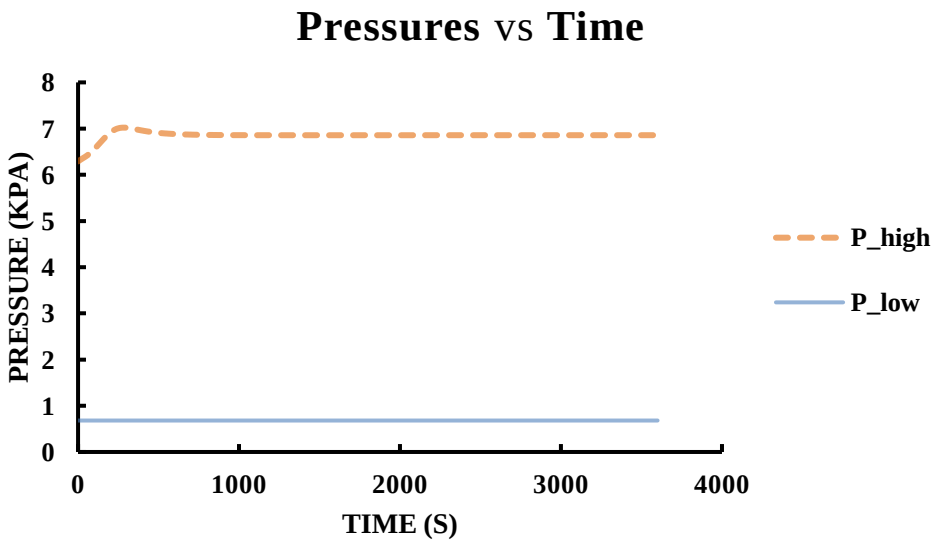

Figure 0.12: Low and high pressures of the cycle.

There are some restrictions that must be taken into account when using Lithium-Bromide/Water pair in an absorption cycle. These restrictions include crystallization, and freezing of the refrigerant. The lower pressure of the cycle is set at 0.68 kPa to avoid freezing of the refrigerant. Subsequently, the high pressure of this cycle takes the balanced tendency as it shown in figure 4.12. The initial high pressure is about 6.4 kPa, then increases slightly by adding heat, then decreases as the concentration inside the generator decreases (fig 4.3), before it stabilizes at operational pressure of 6.86 kPa.

1.15.13 Solution and refrigerant Temperatures change with time:

The fifth set of results pertains to the variation of solution and water vapor temperatures with time.

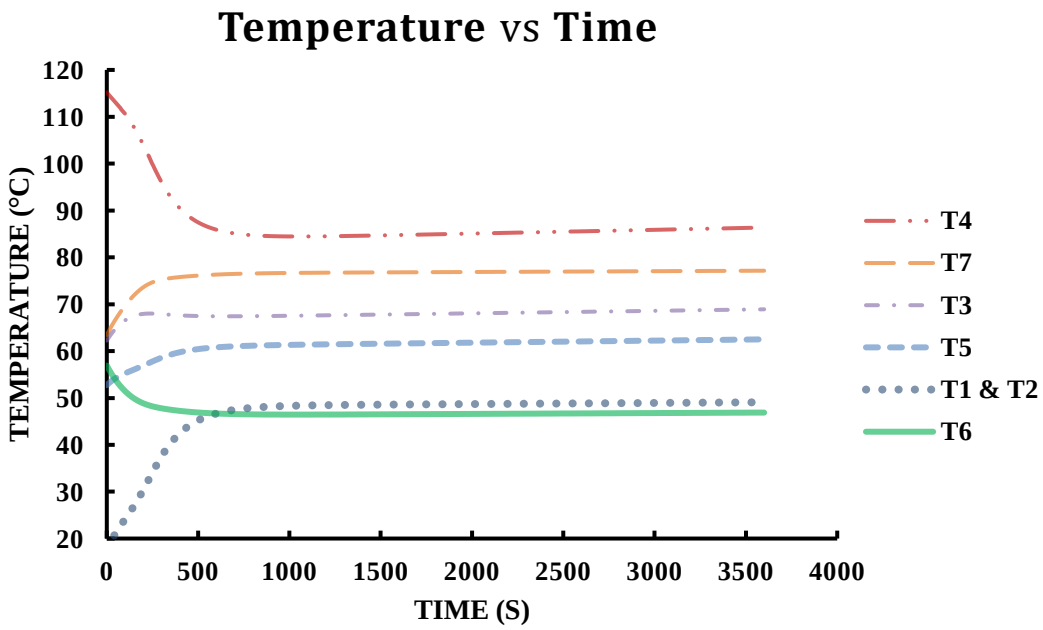

Figure 0.13: Temperatures of the solution and the regenerated refrigerant.

Variation of solution and refrigerant temperatures are shown in figure 4.13. As it can be seen from the figure, refrigerant temperature at the exit of the generator (state 7), temperature of the weak solution before and after the heat exchanger (state 1,2 and 3), and temperature of the strong solution after it passes the heat exchanger (state 5) increase gradually during the incipient period, before they nearly stabilize at particular values.

Since the temperature and enthalpy are correlated; the variation of solution temperature has similar decreasing trend as the variation of solution enthalpy at the exit of the generator

(state 4), which is the same variation of enthalpy of the solution inside the generator (figure 4.4). An opposite increasing variation in temperature happens for the solution inside the absorber, and hence for the solution at suction side of the pump. The pumping process has negligible effect in temperature of the solution, consequently, the variation of temperature of the solution in suction (states 1) and delivery (states 2) sides of the pump are identical (figure 4.13).

1.16 Crystallization and optimal initial condition

Crystallizing or freezing up of lithium-bromide is a serious problem in lithium bromide/ water absorption systems. The mechanism of failure is that, the lithium-bromide/water solution becomes so concentrated and when the solution temperature decreases; lithium bromide crystals form and plug the machine. Each concentration has a corresponding crystallization temperature below it crystallization will take place.

In absorption cooling systems, crystallization is most likely to occur in the lithium-bromide/water solution before it enters to the absorber “at state 6 in Figure 3.2” where the strong solution has the lowest temperature. Thus, it is essential to keep track of the changeable properties (specifically, the temperature and concentration) there during the transient operation; to ensure avoiding crystallization at any moment until the system reach its safe operating conditions at steady state operation. Table (4.4) list the crystallization status at different time-steps for the solution before it enters to the absorber. As it obvious in table (4.4), crystallization will take place in the system specially at the commencement of the operation.

Table 0.4: Crystallization temperatures of the working solution at point (6) at different time-steps.

			Without considering the inertia			Considering the inertia	
Step	**Concentration %**	**Crystallization Temperature (°C)**	**Temperature (°C)**	**Crystallization status**		**Temperature (°C)**	**Crystallization status**
1	69	90.7	86.04	Occurs		56.91	Occurs
2	68	79.53	76.23	Occurs		55.11	Occurs
3	67	67.6	69.47	Avoided	Safe Range	53.33	Occurs
4	66	54.76	57.68	Avoided		51.52	Occurs
5	65	41.27	52.34	Avoided		49.76	Avoided
6	64	38.22	48.98	Avoided		48.08	Avoided
7	63	34.95	46.48	Avoided		46.48	Avoided

Safe Range

Accordingly, it is essential to optimize the initial solution concentrations values to avoid the risk of crystallization.

A prepared solution with lithium bromide concentration of 69-70% by mass is susceptible to form precipitation of salt. Thus, solution with lesser percentages of the absorbent should be used initially to avoid crystallization. Figure 4.14 show the change of solution properties (Concentration, Temperature, and Crystallization temperatures) before it enters the absorber with time after optimizing the initial value of solution concentration. It can be clearly seen that, solution temperatures are always greater than crystallization temperatures which means no formation of lithium bromide salts within the system and hence the operation will be safe at any time.

The safe point in which crystallization phenomenon is just avoided is affected by the thermal inertia. Crystallization becomes more sensitive when the thermal inertia is taken

into consideration as it is obvious in the table. When the thermal inertia is neglected the safe operation starts when the concentration is 67%, while, if the inertia is taken into account the operation will not be safe unless the concentration is 65% or less.

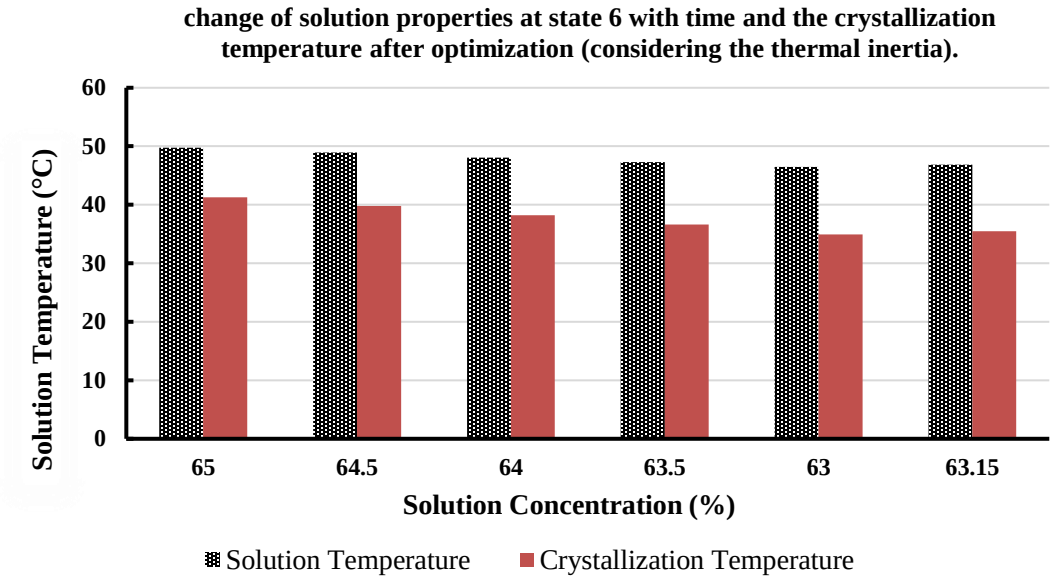

Figure 0.14: optimized solution properties before it enters the absorber with time.

Furthermore, the crystallization risk at all points in the solution cycle was checked out and the observations are listed in (table 4.5). The strong solution (concentration of 63.15%) has corresponding crystallization temperature of 32.22 °C, and its temperatures at points 4, 5, and 6 are greater, which means no risk of crystallization. On the other side, the crystallization temperature associated with the weak concentration (concentration of 57.03 %) is 1.989 °C, which also imply safe operation as the temperatures at points 1, 2, and 3 reported greater values than this crystallization temperature. Eventual solution cycle is plotted in Figure 4.15.

Table 0.5: Crystallization temperatures of the working solution at various positions in the cycle.

Position on the cycle	Concentration %	Temperature (°C)	Crystallization Temperature (°C)	Status
1	57.03	49.08	1.989	Safe
2	57.03	49.08	1.989	Safe
3	57.03	68.92	1.989	Safe
4	63.16	86.37	32.22	Safe
5	63.16	62.51	32.22	Safe
6	63.16	46.88	32.22	Safe

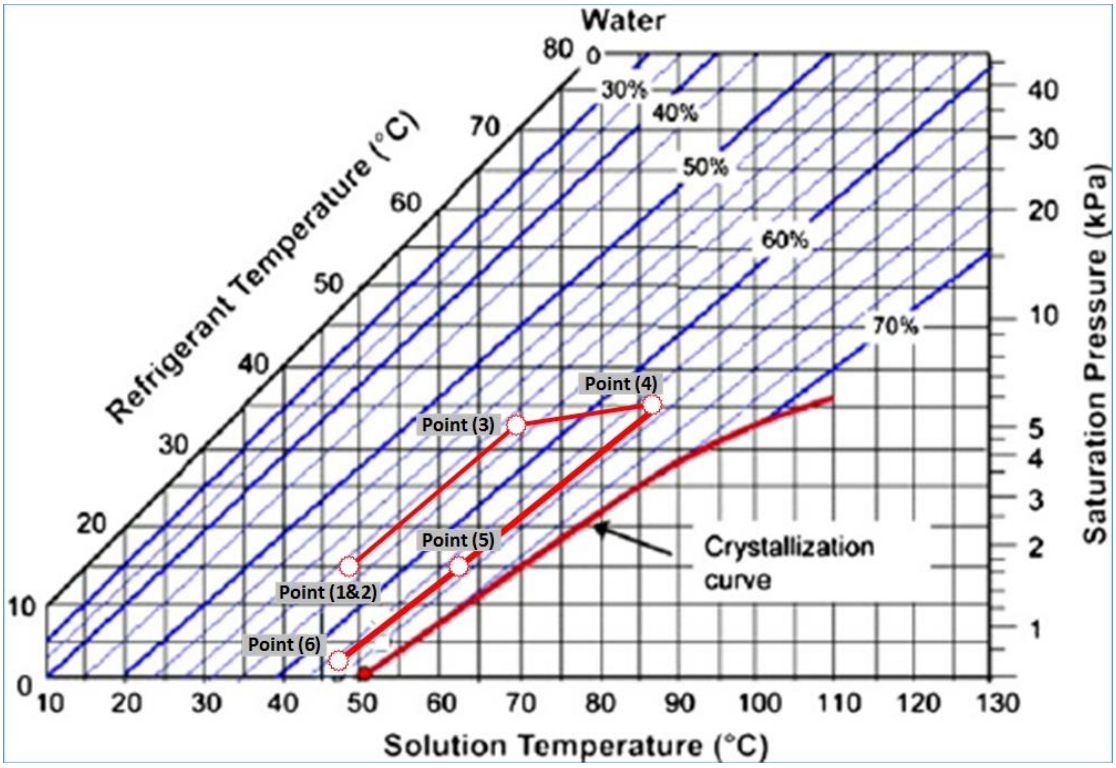

Figure 0.15: Dühring plot for the LiBr/H_2O cycle at steady state operation.

1.17 Effect of applying different heat inputs on the performance of the absorption cooling cycle:

The set of results in this section pertains to the variation of refrigerant regeneration rate and coefficient of performance of the cycle with time for different values of heat inputs. The change of refrigerant regeneration rate with time under different values of heat inputs supplied to generator is shown in figure 4.16.

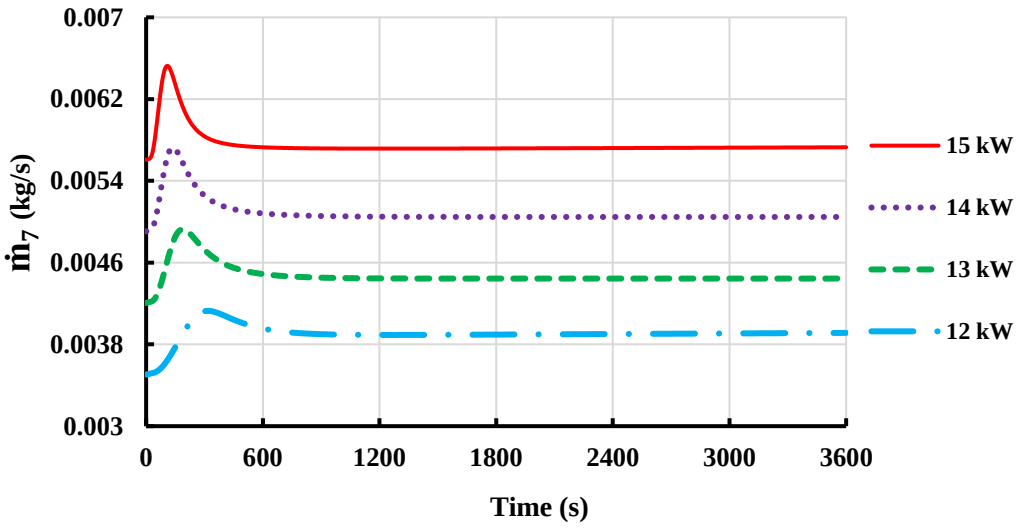

Figure 0.16: Variation of regenerated refrigerant with time for different heat inputs.

It is axiomatic that the rate of desorbing the refrigerant from the solution in the desorber is directly proportional to the heat input. Moreover, figure (4.16) demonstrates that, with increasing heat input the generation of the refrigerant develops faster and greater at the commencement of the operation, before it stabilizes at a certain rate with higher rate for the greater heat input. Furthermore, with increasing the heat input the absorption cycle reaches the steady state in a shorter period of time. This is because the shorter warming-up and fluctuation operation period, and all parameters reach operating condition faster.

Figure (4.17) shows the variation of coefficient of performance of the cycle with time for different values of heat inputs.

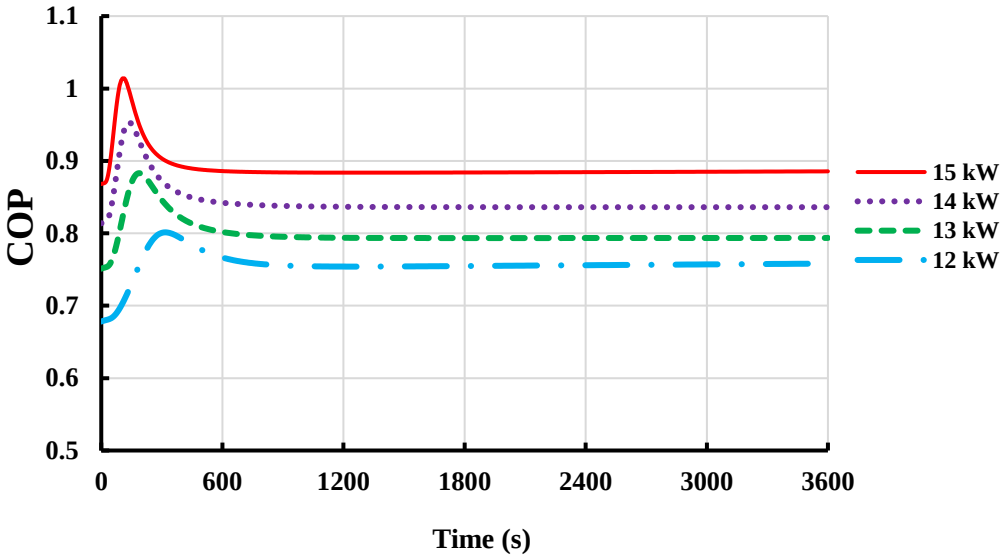

Figure 0.17: Variation of COP with time for different heat inputs.

The thermal COP of the absorption cycle is the ratio between the cooling output and heat input in the desorber. The variation of the COP has similar trend as the variation of refrigerant regeneration rate. That is because the lower pressure is fixed at a certain value and thus the COP depends on the rate of refrigerant regeneration which itself proportions to the heat inputs.

1.18 Considering the inertia of desorber and absorber:

Previously, the inertia of all components was not taking into account, however, in real life it is considerable. In reality, the inertia of the desorber and absorber are very huge compare to the other components of the absorption chiller. Thus, in order to simplify the problem, in this section the inertia of the absorber and desorber is taken into consideration, while the inertia of the other components is not considered.

The governing equations becomes as follow:

Energy balance in the desorber:

$$\frac{d(U_G)}{dt} = \frac{d}{dt}(M_s.u_s + M_{st}.u_{st})_G = \frac{d}{dt}\left((M_s.C_{p_s} + M_{st}.C_{p_{st}})_G(T_G)\right) \quad (4.2)$$

Energy balance in the absorber:

$$\frac{d(U_A)}{dt} = \frac{d}{dt}(M_s.u_s + M_{st}.u_{st})_A = \frac{d}{dt}\left((M_s.C_{p_s} + M_{st}.C_{p_{st}})_A(T_A)\right) \quad (4.3)$$

The set of results in this section pertains to the effect of taking into account the inertia of the desorber and absorber on regeneration rate and coefficient of performance of the cycle with time. The change of refrigerant regeneration rate and the coefficient of performance with time in case of considering the inertia of the absorber and the desorber are represented by the dashed curves in figures 4.18 and 4.19.

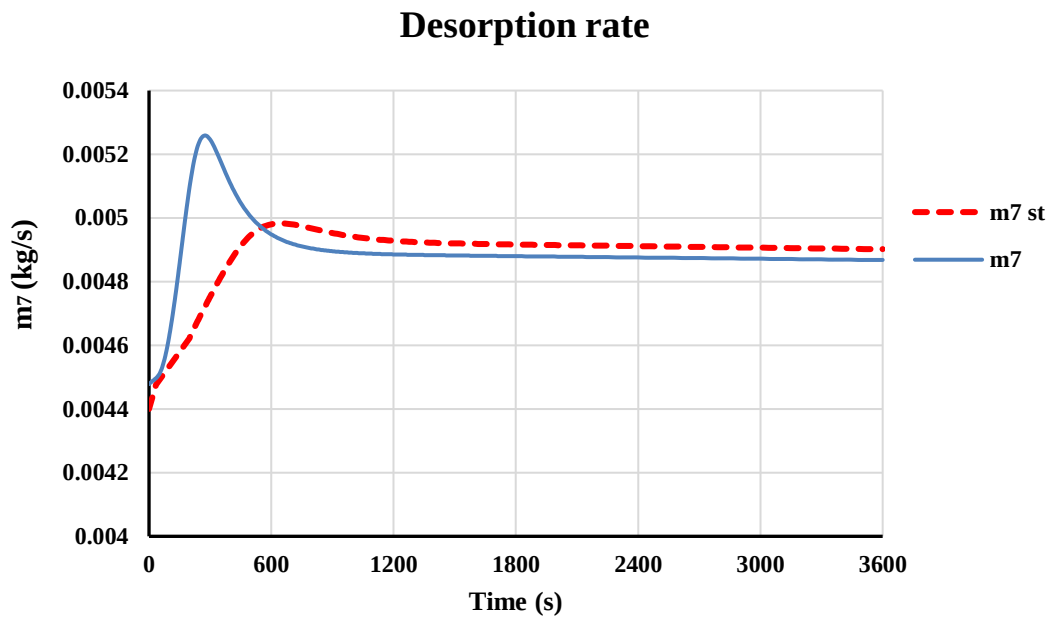

Figure 0.18: Effect of the inertia on the variation of desorption rate with time.

Figure 4.18 shows the desorption rate of the refrigerant with time. The figure demonestrats that the cycle takes about 1200 seconds to reach the steady state compare to 840 seconds when the inertia of the components is neglected. This difference attributes to the thermal mass of generator structure. Consequently, the inertia of the components has a considerable effect, and it should be taken into account when it comes to model the absorption refrigeration cycles. Also, this effect is obvious in figure (4.19) which shows the variation of coefficient of performance of the cycle with time in case of considering effect of the inertia in compare with the case of neglecting the inertia.

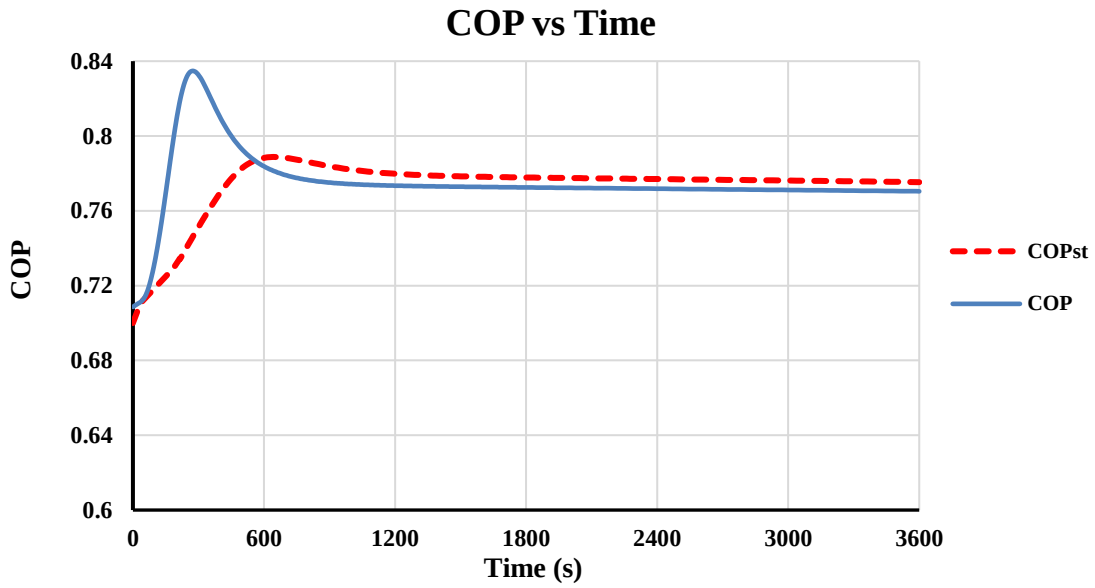

Figure 0.19: Effect of the inertia on the variation of COP with time.

The thermal COP of the absorption cycle is the ratio between the cooling output and heat input in the desorber. The variation of the COP has similar trend as the variation of refrigerant regeneration rate. Due to the thermal masses of the generator and the absorber the chiller takes longer time to reach the operating condition in the steady state operation.

1.19 Assessment of performance of solar absorption cooling system:

This section studies the performance of the solar absorption system when installed in Dhahran, Saudi Arabia.

1.19.1 Meteorological data of a representative day of summer in Dhahran – KSA:

A representative day (11th of June) was selected among other summer days which was found to be in conformance with the behavior of summer. The meteorological data is of this day is shown in figure (4.18).

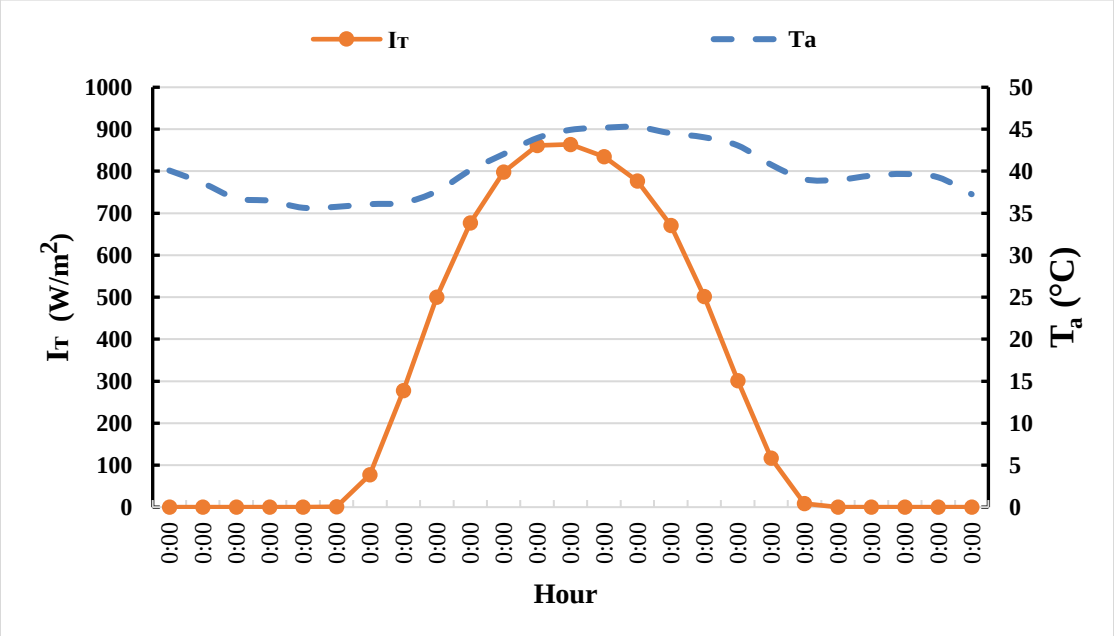

Figure 0.20: Average hourly solar irradiance & ambient temperature for representative day (11th of June) in Dhahran, KSA.

The temperature of the representative day ranges from 35 to 45° C throughout the whole day, with an average hourly solar radiation that peaks at 864 W/m^2 at noon. Naturally, the hourly solar radiation falls to a zero value from 7 PM (sunset) to 5 am (sunrise).

1.19.2 Sizing of a solar collector to drive the cooling absorption system:

An evacuated tube solar collector operating in Dhahran-Saudi Arabia (Longitude 50 E, Latitude 26.3° N), using meteorological data of a representative summer day (11th of June) is considered to drive the absorption cooling system in order to cover a cooling load of 3 TR (which is the minimum cooling effect to be produced by the given absorption system that prevent subzero temperature at the evaporator). The collector performance could be determined by using the following formulas [38]:

$$Q_u = F_R . A_c . (I * \tau\alpha - U(T_{w_i} - T_a)) \quad (4.1)$$

$$F_R = F'' * F' \quad (4.2)$$

$$F'' = \frac{\dot{m}_w C_w}{A_c U F'} \left[1 - \exp\left(-\frac{A_c U F'}{\dot{m}_w C_w}\right)\right] \quad (4.3)$$

The collector has a mass flow rate of 0.025 kg/s.m^2, inlet temperature varies from 80 to 84.5° C, and other typical values of some parameters as listed in table (4.6) [24].

Table 0.6: Typical values of some parameters used in sizing of the solar collector [23].

SPECIFICATION	VALUE
τα	0.86
U $_{overall}$	8 W/m^2
F'	0.841
Circulating fluid	water
$\dot{m}_w$	0.025 kg/s.m^2
c_w	4190 J/kg. K

The performance of the solar collector individually and the combined solar absorption system were investigated under meteorological data of Dhahran on 11th of June and the results are listed in tables (4.7) and (4.8) respectively for a collector area of 40 m^2. The investigation was carried out between 8:00 and 5:00 pm because it is the only period that the solar collector can produce considerable amount of useful heat gain.

Table 0.7: Performance of the collector during the effective period (from 8:00 am to 5:00 pm).

Time	***I***	T_a	Q_u	η_c
Hour	W/m^2	*°C*	*kW*	*%*
8:00 – 9:00	500.5	37.61	1.783	8.905
9:00 – 10:00	676.8	40.12	7.748	28.62
10:00 – 11:00	798.1	42.04	11.91	37.3
11:00 – 12:00	861	43.95	14.32	41.57
12:00 – 13:00	864	44.93	14.68	42.47
13:00 – 14:00	835	45.18	13.88	41.56
14:00 – 15:00	776.5	45.26	12.16	39.14
15:00 – 16:00	670.6	44.52	8.786	32.75
16:00 – 17:00	502	44.04	3.615	18

The solar collector is not capable of providing the absorption system with enough heat to produce a cooling effect between 8:00 to 9:00 am. However, more than 14 kW could be delivered around noon enabling the absorption system to produce up to 3 TR between 12:00 and 1:00 pm.

Table 0.8: Performance of the solar-absorption cooling system (8:00 am to 5:00 pm).

Time	Q_g	Q_e	***COP***
Hour	*kW*	*kW*	
8:00 – 9:00	1.783	-	-
9:00 – 10:00	7.748	5.667	0.731
10:00 – 11:00	11.91	8.672	0.728
11:00 – 12:00	14.32	10.334	0.722
12:00 – 13:00	14.68	10.579	0.721
13:00 – 14:00	13.88	10.034	0.723
14:00 – 15:00	12.16	8.847	0.728
15:00 – 16:00	8.786	6.435	0.732
16:00 – 17:00	3.615	2.457	0.680

Additionally, to obtain 3 TR cooling effect produced by the absorption cooling system, the desorber must be supplied by a heat rate of 14.67 kW from the solar system. For a solar collector of an area of 40 m^2, the solar system is not capable to satisfy this amount of the required power except at the hour immediately after noon (i.e. from 12:00 to 13:00) due to the intensive solar radiation during this hour. Here, the term Solar Fraction (SF) is introduced to identify the amount of energy to be provided by an auxiliary system to cover the shortage in energy that should be delivered to the absorption system to achieve an output of 3 TR. Solar Fraction is the ratio between the amount of energy delivered by a solar system to the total energy that should be delivered. Figure (4.19) shows the variation of solar fraction throughout the effective operation period (from 8:00 to 5:00 pm) for different areas of solar collector.

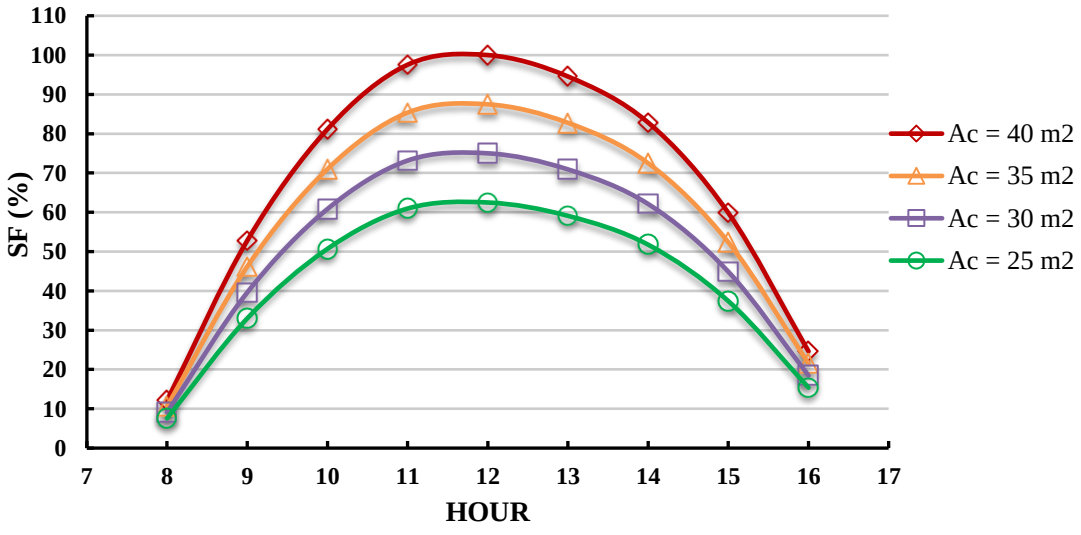

Figure 0.21: Solar fraction during effective operation time for different collector areas.

There are small amounts of solar radiation during the earlier and latter hours of the day; the solar system produces around 10% of total energy required for the system to produce 3 TR cooling effect in those hours, the remainder 90% of the total energy required should be covered with an auxiliary power source. Nevertheless, the only case of which the system doesn't require an auxiliary power source is from 12 to 1 pm with a solar collector area of a 40 m^2.

If however the auxiliary system is not used to provide the rest of the total required energy, the area of the solar collector should follow the trend shown in figure (4.20). This solution however suggests the use of around 329 m^2 of area in the time range from 8 am to 9 am to provide the system with the needed energy which is economically and spatially infeasible.

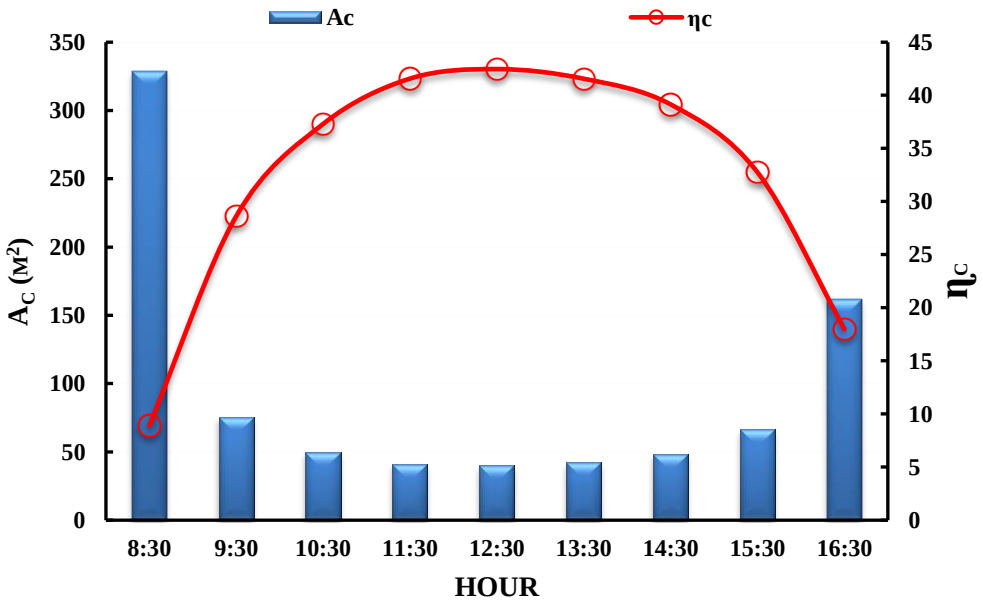

Figure 0.22: Collector area and efficiency required drive 3 TR absorption system installed under Dhahran climate condition on 11th of June.

CHAPTER 5

CONCLUSION AND RECOMMENDATION

A transient thermodynamic analysis has been performed on a single stage lithium-bromide/water absorption cooling cycle assumed to be powered by constant input power from a solar field. The major focus was on the transient period that precedes steady-state period. A set of initial conditions were introduced and optimized in a way that always keeps the absorbent concentration in safe level without any risk of crystallization. Each component had been elucidated individually and its governing equations has been elicited before combining all of them to build the model. The analysis results indicate a transient period of 840 seconds before the dynamic terms vanish and the cycle reaches the steady-state. Moreover, most parameters develop from their initial values steadily before they reach their peaks and then decline smoothly to the operating condition. In order to verify the results of the developed dynamic model a comparison was carried out with steady state analysis, and also dynamic simulation results reported in the literature. The comparison indicated a good agreement between the results of this model and the ones from the literature with a maximum difference of 7.2%. This study drew the attention of importance of the initial state when it comes to transient analysis. In order to obtain safe operation, it is essential to keep tracking of the changeable properties of the solution within the cycle and ensure that crystallization will not take place throughout the operation. Furthermore, the effects of the heat input and inertia of the absorber and the desorber on the transient period were considered. The investigation of the system performance under different heat inputs resulted in shorter transient period as the heat input is increased. On the other, when the inertia

of the components was considered, the cycle took about 20 minutes before it reached the steady state operation, and that reflect the importance of taking the inertia of the components into consideration. The developed dynamic model is able to predict the performance of single effect LiBr/H_2O absorption cooling system. Hence, the model can be used in designing appropriate absorption systems for various applications and while ensuring safe operation.

Thereafter, the performance of the solar absorption system was investigated under meteorological condition of Dhahran – Saudi Arabia for a representative day of summer. The effective period during which the solar system produces a considerable amount of useful heat gain is from 8:00 am to 5:00 pm. The results indicate that; an auxiliary heating system is needed to assist the solar system in order to empower the absorption cooling system by 14.67 kW required to cover a cooling load of 3 TR. The Solar fraction ranges between 60 to 90% during noon times for collector areas between 25, and 35 m^2. Nevertheless, the evacuated tube collector is able to satisfy the total required energy alone during the hour immediately after noon if the collector area is 40 m^2 (SF = 100%).

It is highly recommended to conduct further studies on such cycles for the purpose of reducing such assumptions, and trying to generalize the simulation by introducing the solar field into the dynamic model seeking for inclusive model that combine the transient behavior of the solar field and the consequence unsteady response of the absorption cooling cycle seeking for a deeper understanding of such combined systems.

References

[1] P. Srikhirin, S. Aphornratana, and S. Chungpaibulpatana, "A review of absorption refrigeration technologies," *Renew. Sustain. Energy Rev.*, vol. 5, no. 4, pp. 343–372, 2000.

[2] M. M. Fernández, "Solar cooling of buildings in a Swedish climate Analysis and design of solar cooling in Building 45 at Högskolan i Gävle .," 2014.

[3] a. Buonomano, F. Calise, and a. Palombo, "Solar heating and cooling systems by CPVT and ET solar collectors: A novel transient simulation model," *Appl. Energy*, vol. 103, pp. 588–606, 2013.

[4] B. Kim and J. Park, "Dynamic simulation of a single-effect ammonia-water absorption chiller," *Int. J. Refrig.*, vol. 30, no. 3, pp. 535–545, 2007.

[5] Z. O. Hovsapian, "Florida State University Libraries Thermodynamic Optimization of a Solar System for Cogeneration of Water Heating / Purification and Absorption Cooling," 2009.

[6] Y. Hu, "Advanced Exergy Analysis for a Solar Double Stage Absorption Chiller Advanced Exergy Analysis for a Solar Double Stage Absorption Chiller," 2012.

[7] I. Shesho, "Analysis and design of solar based systems for heating and cooling of buildings," no. July, 2014.

[8] S. S. Ahmedullah, "Integrated Solar Energy and Absorption Cooling Model for Hvac (Heating, Ventilating, and Air Conditioning) Applications in Buildings," pp. 43–46, 2006.

[9] C. Carlson, M. Coulter, C. Kunkle, and P. Watson, "Solar absorption chiller," 2014.

[10] Y. Hang and M. Qu, "The impact of hot and cold storages on a solar absorption cooling system for an office building," *Int. High Perform. Build. Conf.*, p. 9, 2010.

[11] A. Hirai, "Solar Cooling System Using Solar-Driven Hybrid Chiller," *Int. Refrig. Air Cond.*, pp. 1–9, 2012.

[12] M. Jahandardoost, "simulation of an air cooled single effect solar absorption cooling system with evacuated tube collectors by Mohsen Jahandardoost Bachelor of Science in Mechanical Engineering University of Guilan A thesis submitted in partial fulfillment of the requiremen," 2014.

[13] and M. A. B. Çengel, Yunus A., *Thermodynamics: An Engineering Approach*, 5th ed. Boston: McGraw-Hill, 2001.

[14] H. Performance and R. Computer, “Carnegie mellon university,” 2001.

[15] M. Naji and I.- Jordan, “(Communicated by J.P. Hartnett and W.J. Minkowycz),” *Analysis*, vol. 28, no. 6, pp. 835–845, 2001.

[16] A. Arsalis and A. N. Alexandrou, “Parametric study and cost analysis of a solar-heating-and-cooling system for detached single-family households in hot climates,” *Sol. Energy*, vol. 117, pp. 59–73, 2015.

[17] A. Acuña, F. Lara, N. Velázquez, and J. Cerezo, “Optimum generator temperature to couple different diffusion absorption solar cooling systems,” *Int. J. Refrig.*, vol. 45, pp. 128–135, 2014.

[18] Z. Li, X. Ye, and J. Liu, “Optimal temperature of collector for solar double effect LiBr/H2O absorption cooling system in subtropical city based on a year round meteorological data,” *Appl. Therm. Eng.*, vol. 69, no. 1–2, pp. 19–28, 2014.

[19] A. Ghafoor and A. Munir, “Thermo-economic Optimization of Solar Assisted Heating and Cooling (SAHC) System,” *Int. J. Renew. Energy Dev.*, vol. 3, no. 3, pp. 217–227, 2014.

[20] D. Micallef and C. Micallef, “Mathematical model of a vapour absorption refrigeration unit,” *Int. J. Simul. Model.*, vol. 9, no. 2, pp. 86–97, 2010.

[21] V. Mittal, K. S. Kasana, and N. S. Thakur, “Modelling and simulation of a solar absorption cooling system for India,” *J. Energy South. Africa*, vol. 17, no. 3, pp. 65–70, 2006.

[22] P. Zadeh, “the energy and exergy ch Ar ch,” *Mech. Eng.*, vol. 4, no. 4, 2011.

[23] B. Le Lostec, J. Millette, and N. Galanis, “Finite time thermodynamics study and exergetic analysis of ammonia-water absorption systems,” *Int. J. Therm. Sci.*, vol. 49, no. 7, pp. 1264–1276, 2010.

[24] M. Ozgoren, M. Bilgili, and O. Babayigit, “Hourly performance prediction of ammonia-water solar absorption refrigeration,” *Appl. Therm. Eng.*, vol. 40, pp. 80–90, 2012.

[25] A. Iranmanesh and M. a Mehrabian, “Transient Characteristics of a Single-Effect Absorption Refrigeration Cycle,” *J. Energy Eng. Manag.*, vol. 2, no. 4, pp. 40–47, 2012.

[26] O. Marc, F. Sinama, J.-P. Praene, F. Lucas, and J. Castaing-Lasvignottes, “Dynamic modeling and experimental validation elements of a 30 kW LiBr/H2O single effect absorption chiller for solar application,” *Appl. Therm. Eng.*, vol. 90, pp. 980–993, 2015.

[27] W. Cai, M. Sen, and S. Paolucci, “Dynamic Simulation of an Ammonia À water Absorption Refrigeration System,” pp. 2070–2076, 2012.

[28] T. He, X. Zhang, C. Wang, M. Wang, B. Li, N. Xue, K. Shimizu, K. Takahashi, and Y. Wu, “Application of Solar Thermal Cooling System Driven by Low Temperature Heat Source in China,” *Energy Procedia*, vol. 70, pp. 454–461, 2015.

[29] F. Calise, M. Dentice d’Accadia, and a. Palombo, “Transient analysis and energy optimization of solar heating and cooling systems in various configurations,” *Sol. Energy*, vol. 84, no. 3, pp. 432–449, 2010.

[30] A. Budania, S. Ahmad, and S. Jain, “Transient simulation of a solar absorption cooling system,” *Int. J. Low-Carbon Technol.*, pp. 1–7, 2013.

[31] A. Syed, M. Izquierdo, P. Rodríguez, G. Maidment, J. Missenden, A. Lecuona, and R. Tozer, “A novel experimental investigation of a solar cooling system in Madrid,” *Int. J. Refrig.*, vol. 28, no. 6, pp. 859–871, 2005.

[32] C. V Vazhappilly, T. Tharayil, and a P. Nagarajan, “Modeling And Experimental Analysis Of Generator In Vapour Absorption Refrigeration System,” vol. 3, no. 5, pp. 63–67, 2013.

[33] M. Izquierdo, A. González-Gil, and E. Palacios, “Solar-powered single-and double-effect directly air-cooled LiBr-H2O absorption prototype built as a single unit,” *Appl. Energy*, vol. 130, pp. 7–19, 2014.

[34] C. B. Dorgan, C. E. Dorgan, and A. Leight, “No Title,” in *“Ashrae’s New Application Guide for Absorption Cooling/refrigeration Using Recovered Heat.,”* 1995, p. 37.7.

[35] G. Grossman, “Solar-powered systems for cooling, dehumidification and air-conditioning,” *Sol. Energy*, vol. 72, no. 1, pp. 53–62, 2002.

[36] G. Evola, N. Le Pierrès, F. Boudehenn, and P. Papillon, “Proposal and validation of a model for the dynamic simulation of a solar-assisted single-stage LiBr/water absorption chiller,” *Int. J. Refrig.*, vol. 36, no. 3, pp. 1015–1028, 2013.

[37] K. E. Herold, R. Radermacher, and S. A. Klein, *Absorption Chillers and Heat Pumps*, Second Edi. Boka Raton, New York, London, Tokyo: CRC Press Inc., 1996.

[38] J. a. Duffie, W. a. Beckman, and W. M. Worek, *Solar Engineering of Thermal Processes, 4nd ed.*, vol. 116. 2003.

Appendix

Summary of the literature review:

Authors, reference No., (publication year)	**Working Solution**	**Heat Source**	**Auxiliary & Storage Systems**	**Nominal Capacity**	**Accomplishment & Remarks**
A. Syed, *et al*., [31], (2005)	$LiBr/H_2O$	Solar energy	2 m^3 stratified hot water storage tank	35 kW	• Max cooling capacity of 7.5 kW with 0.6 max instantaneous COP was recorded. • The experiment results is considered as a benchmark.
B. Le Lostec, *et al*., [23], (2010)	H_2O-NH_3	Electric power	-	3 kW	• Simulation based on finite time. • Assumed steady state. • Different parameters were assumed constant. • Exergitic analysis (EX_d is 33% in the absorber, 34% in the generator) were conducted.

F. Calise, *et al*., [29], (2010)	$LiBr/H_2O$	Solar energy	Boiler	157 kW	• Transient simulation model. • Three different configurations. • An economic model was also developed and indicated that such systems are usually unprofitable.
V. Mital *et al.*, [21], (2006)	$LiBr/H_2O$	Solar energy	-	-	• Came up with simple linear mathematical model. • Validated with example from *ASHRAE Fundamentals Handbook.* • Did not take into consideration the transient behavior.
Micallef, D. and Micallef, C., [20], (2010)	Either $LiBr/H_2O$ Or H_2O-NH_3				
W. Cai, *et al*., [27], (2010)	H_2O-NH_3	High T source	-	320 kW	• Used equation of state to extract thermodynamic properties. • Pressure rise across the pump by step of 1% increased NH_3 flow rate, cooling effect, and COP speedily. • Time for steady state was 1 minute

M. Ozgoren, *et al.*, [24], (2011)	H_2O-NH_3	Solar energy	-	3.5 kW	• Experimental investigation on hourly basis. • The best performance was recorded for generator temperature of 110 °C or higher. • Mostly, during the day the COP ranged between 0.243-0.454 and 1.243 to 1.454 for cooling and heating respectively. • The results indicated that the solar absorption system is suitable for residential and office buildings especially during daytime
F. Zadeh, and N. Bozorgan, [22], (2011)	LiBr/H_2O	Any high T heat source	-	1360 kW	• A code in EES software has been developed. • The results indicated that the generator and absorber encompass the highest exergy destruction. • Performing exergy analysis is recommended in designing an absorption system; because it precisely identifies real losses.
A. Iranmanesh, and M. Mehrabian, [25], (2012)	LiBr/H_2O	Any high T heat source	-	-	• Applied a lumped-parameter model to make a dynamic simulation using EES & MATLAB. • EES was used to extract the thermodynamic properties in order to avoid inaccuracy. • What was new is "considering the impact of quality on the solution concentration at the outlets of absorber and generator". • COP and exergetic efficiency decline with time, to reach the steady state values. Transient exergy analysis was carried out.

A. Budania, *et al*., [30], (2013)	$LiBr/H_2O$	Solar energy	auxiliary heating & hot water storage tank	105.5 kW	• Modelling & simulation using TRNSYS. • The output of the system increased with the collector area, nonetheless, it was restricted by the capacity of the storage tank owing to the maximum water temperature allowed. • For the system controls; with auxiliary heating, when the storage tank capacity increased, the average output cooling potential decreased because of the lower water temperature.
C. V. Vazhappilly, *et al.*, [32], (2013)	H_2O-NH_3	Exhaust -gases from an IC engine.	-	350 kW	• Generator system _ or the heating coil_ was substituted by frame-plate type heat exchanger.
Tao He, *et al.* , [28], (2014)	$LiBr/H_2O$	Solar energy	Heating storage tank & bio mass boiler	175.8 kW	• Modeled a solar thermal cooling system. • Optimization was implemented by using TRNSYS. • The results were validated experimentally. • An annual average collector efficiency equal to 37.6% with consequent solar fractions 0.76 and 0.38 in summer and winter respectively were obtained. • Compared to conventional system 66% of energy consumption was reduced. The modelled system has 5 years payback period.

A. Ghafoor and A. Munir , [19], (2014)	$LiBr/H_2O$	Solar energy	Backup auxiliary heating system "gas boiler"	60 kW	• Sensitivity analysis of heating-cooling system. • Maximization of net positive value was used to calculate the economic feasibility. • To have cost beneficial system, financial incentives are needed. • Solar fraction might reach 55 to 100% for cooling during summer, and 87 to 100% for heating during winter.
Z. Li *et al.* , [18], (2014)	$LiBr/H_2O$	Solar energy	-	20 kW	• Double effect system. • Primarily focused on the response of the system performance with the collector temperature. • A monthly basis climatological data was used in the simulation to develop a parametric model. • Optimum range of collector inlet temperature is 110-130°C. • If the system involve a hot water storage unit; the optimal inlet temperature becomes higher.
M. Izquierdo, *et al.*, [33], (2014)	$LiBr/H_2O$	Solar energy	1.5 m^3 hot water storage tank	4.5 kW	• Design and built a prototype able to operate interchangeably between single effect (4.5 kW) and double-effect unit (7 kW). • Single effect mode satisfy 65% of the seasonal cooling load. • Double effect mode can satisfy the total load but it needs to warm up a thermal oil up to the operating temperature of the high pressure generator.
		Thermal oil.		7 kW	

A. Acuna, *et al.*, [17], (2014)	NH_3/LiO_3 And NH_3/ NaSCN	Solar energy	-	-	• Found out the best generator temperatures to produce maximum efficiencies. • The optimal coupling temperatures vary between 70 to 150 °C. • Different types of solar collectors were examined. • The best configuration was when NH_3-$LiNO_3$ is used, and the system was driven by evacuated tube collectors. • Steady state assumption.
A. Arsalis, and A. Alexandru, [16], (2015)	$LiBr/H_2O$	Solar energy	an auxiliary heating system is connected to the hot water storage unit	18.3 kW	• Prepared a design and model for solar heating/cooling system. • Optimization results were 70 m^2 as a collector area and hot water storage tank capacity of 7 m^3 to achieve optimum solar system combination to drive the heating/cooling system. • Overall cost was $3,719. • Unless the cost of the solar collector is over $360/$m^2$; the SHC system would be preferable over electric heat pump systems.

Olivier Marc, *et al.*, [26], (2015)	$LiBr/H_2O$	Solar energy	-	30 kW	• Clear dynamic model. • The experiment validation results are quite acceptable, particularly in the outlet temperature of each component. • The model is used to optimize the thermal COP for three different levels of cooling capacities. • The results indicated that "it is better to have lower inlet temperature in the absorber than having higher inlet temperature in the generator".

Vitae

Name	:HAMZA KAMAL ALI MUKHTAR
Nationality	:SUDANESE
Date of Birth	:4/1/1992
Email	:MEZO085@HOTMAIL.COM
Address	:P.O.BOX 5040, CORE-RE, RI, 31261, Dhahran, KSA
Academic Background	:B. E . MECHANICAL ENGINEERING (SEP 2013)
	:UNIVERSITY OF KHARTOUM
	:KHARTOUM, SUDAN